Diana Guerra de Paiva

Licenciatura em Engenharia Biomédica

Liquid Crystalline Microenvironments For Tissue Engineering

Dissertação para obtenção do Grau de Mestre em

Engenharia Biomédica

Orientador: Professor Doutor Pedro Granja, Investigador Principal, INEB - Instituto de Engenharia Biomédica, Universidade do Porto

Co-Orientador: Doutora Susete Fernandes, Investigadora em Pós-Doutoramento, CENIMAT/I3N – Departamento de Ciências dos Materiais, Faculdade de Ciências e Tecnologia da Universidade Nova de Lisboa

Júri:

Presidente: Prof. Doutora Célia Maria Reis Henriques
Arguente: Prof. Doutora Maria Teresa Varanda Cidade
Vogal: Prof. Doutor Pedro Lopes Granja

FACULDADE DE CIÊNCIAS E TECNOLOGIA
UNIVERSIDADE NOVA DE LISBOA

Setembro 2015

Diana Guerra de Paiva

Licenciatura em Engenharia Biomédica

Liquid Crystalline Microenvironments For Tissue Engineering

Dissertação para obtenção do Grau de Mestre em

Engenharia Biomédica

Orientador: Professor Doutor Pedro Granja, Investigador Principal, INEB - Instituto de Engenharia Biomédica, Universidade do Porto

Co-Orientador: Doutora Susete Fernandes, Investigadora em Pós-Doutoramento, CENIMAT/I3N – Departamento de Ciências dos Materiais, Faculdade de Ciências e Tecnologia da Universidade Nova de Lisboa

Júri:

Presidente: Prof. Doutora Célia Maria Reis Henriques
Arguente: Prof. Doutora Maria Teresa Varanda Cidade
Vogal: Prof. Doutor Pedro Lopes Granja

FACULDADE DE CIÊNCIAS E TECNOLOGIA
UNIVERSIDADE NOVA DE LISBOA

Setembro 2015

Liquid Crystalline Microenvironments For Tissue Engineering

Acnowledgements

I want to express my gratitude to Dr. João Paulo Borges, which not being an official supervisor, always helped and guided me; to Dr. Pedro Granja and Dr. Susete Fernandes for the guidance and support they gave to me. Thank you for the knowledge and work skills gave to me and the opportunity to work with different methodologies. I am grateful for the opportunity to perform my thesis in two excellent laboratories: CENIMAT|I3N and INEB – Instituto de Engenharia Biomédica and being kindly received in both. Thank you for the enthusiasm with my work and for your great ideas and support!

At CENIMAT|I3N, besides my co-supervisor, Dr. Susete Fernandes which had the patience to transmit her knowledge and enthusiasm for science, to Dr. Coro Echeverria for her support and help and to Dr. Daniela Gomes for the patient on our Scanning Electron Microscopy session at CENIMAT|I3N.

At INEB I would like to thank to MSc Sara Neves who helped me with her expertise and knowledge in rheology and Dra. Filipa Sousa, who introduced me to cell culture. Thank you both for the sincerity, orientation and suggestions. Thank you Ricardo Vidal, for the advice and collaboration in numerous situations and to all members of the Biocarrier group, which always kindly helped me through the thesis. Thank you to Dra. Paula Sampaio from IBMC (Instituto de Biologia Molecular e Celular) for the help with the Polarized Optical Microscope. To the IBMC Transmission Electron Microscopy technicians, thank you for their help and expertise. At CEMUP (Centro de Materiais da Universidade do Porto), to the Scanning Electron Microscopy technicians thank you for the aid.

I cannot forget of my fellow colleagues and friends both in CENIMAT and INEB who were always there for a conversation and a brief moment of relaxation.

To my friends that accompanied me through this 5 years adventure. To my boyfriend Miguel, who always had the patience to listen in difficult hours and always motivated and supported me. A big thank you.

Last but not least, thank you to my parents and grandmother, which never stopped supporting me in every stage of my life and it is thanks to your love that I am here. Thank you for all your efforts.

Abstract

In this present work, gels with liquid crystalline (LC) phases were studied based on cellulose and collagen. The cellulose was further incorporated in a polymer matrix (polyvinyl alcohol) and in a biocompatible material (glycerol), in order to produce gels with LC phases. The LC phases and other properties of the gels were further investigated in order to determine relationships between structure/properties. Preliminary cellular studies were done to unravel the influence of the LC phase in cell proliferation and the changes in the LC phase due to the presence of the cells.

Nanocrystalline cellulose (NCC) with different aspect ratio, were obtained by acid hydrolysis with sulfuric acid at different reaction times. Gelation of collagen type I was not achieved. The NCC/PVA gels did not presented LC patterns.

NCC/glycerol gels with NCC concentration higher than 7% (w/w) showed, through polarized optical microscopy, a fingerprint texture characteristic of the chiral nematic ordering of the NCC. The pitch of LC phase, increase with the NCC length and no significant variations were observed in gels with higher NCC content. For cell culture studies the 7% (w/w) NCC concentration was selected and the pH of the gels was increased by incubation with culture medium and an increase in the pitch size was noticed. A negative zeta potential of the gels was observed even after pH increase. No chemically modifications were observed by ATR-FTIR after increasing the gels' pH. Preliminary rheological studies gave a good indication of the materials' viscoelastic properties and its thixotropic behaviour. Exploratory cellular tests showed low cell adhesion and cytotoxic tests led to conclude that 48 hours of incubation with culture medium is needed before any cellular studies.

This study shown that the NCC/glycerol gel is a promising material to use in tissue engineering applications.

Keywords: Tissue engineering; Biomaterials; Liquid crystals; "fingerprint" texture; Nanocrystalline cellulose;

Resumo

Neste trabalho, géis com fases liquido-cristalinas (LC) de celulose e colagénio foram estudados. A celulose foi incorporada posteriormente numa matriz polimérica (álcool polivinílico) e num material biocompatível (glicerol). As fases LC, bem como outras propriedades dos géis foram posteriormente estudadas para relacionar as estruturas LC com as propriedades dos géis. Estudos celulares preliminares foram efetuados para determinar a influência da fase LC na proliferação celular e as alterações dessa mesma fase com a presença de células.

Diferentes tempos de hidrólise da celulose com ácido sulfúrico foram efetuados e celulose nanocristalina (NCC) com diferentes comprimentos obtida. A gelificação do colagénio não foi conseguida e os géis de NCC/PVA não apresentaram uma organização liquido-cristalina.

Géis de NCC/glicerol observados por microscopia ótica polarizada (POM), apresentam birrefringência e a partir da concentração de 7%NCC no gel, têm uma textura denominada “impressão digital”, característica da fase LC nemática quiral. O passo dos géis aumenta com o comprimento das NCC. Não se verificou uma variação significativa do passo para concentrações de NCC nos géis mais elevadas. A concentração de 7%NCC foi selecionada para os estudos celulares, tendo o pH dos géis aumentado para incubação com meio de cultura, observando-se o aumento do passo dos géis. Verificou-se um potencial zeta negativo tanto nos géis com e sem incubação em meio de cultura. Por ATR-FTIR não se observaram alterações significativas dos géis após aumento de pH. Com estudos reológicos preliminares, foi possível caracterizar as propriedades viscoelásticas e a tixotropia do material. Testes celulares preliminares demonstraram fraca adesão celular aos géis, contudo testes de citotoxicidade revelaram a necessidade de 48 horas de incubação dos géis antes de qualquer estudo celular.

Este trabalho demonstrou que géis de NCC/glicerol são promissores para serem utilizados em engenharia de tecidos.

Palavras-chave: Engenharia de tecidos; Biomateriais; Cristais líquidos; textura “fingerprint”; Celulose nanocristalina.

Considerations

In nature, cellulose and collagen are one of the most common macromolecules that form liquid crystalline phases. It is believed that liquid crystal phases have a key role in tissue differentiation and is an aim of this thesis to prove this theory. [1] Previous works had shown the importance and the applicability of liquid crystals such as a thermotropic liquid crystals suitable for growth of mammalian cells [2][3] and the alteration of the liquid crystal conformation in the presence of certain chemical substances or physical changes. [4] The main goal of this thesis was to prepare liquid crystalline gels based on nanocrystalline cellulose and collagen. Physical and chemical characterizations of the gels were done and preliminary rheological and cellular studies were performed.

The research performed during this thesis was conducted in two different institutions: DCM – *Departamento de Ciências dos Materiais* at Faculdade de Ciências e Tecnologia, Universidade Nova de Lisboa (FCT/UNL) in the group SBM – CENIMAT|I3N and INEB – Instituto de Engenharia Biomédica at Universidade do Porto (UP) in the group BIOCARRIER.

Chapter I brings an overview of the state of the art of the use of liquid crystals in tissue engineering as well as their theoretical principles. It also introduces the main materials used during the experimental part of the thesis and its current usages in the tissue engineering field.

Chapter II describes the preparation of the studied biomaterials as well as, the characterization techniques and studies performed on the samples (physical, chemical and biological characterization, as well as, rheological experiments).

In the Chapter III the results obtained were presented and discussed.

Chapter IV presents the overall conclusions and chapter V presents the future directions that can be studied and explored in future works. An annex complements some theoretical principles to better understand the rheological experiments.

Contents

List of figures

List of tables

Abbreviations

LCs – Liquid Crystals

NCC – Nanocrystalline Cellulose

LCTFs – Liquid Crystal Tunable Filters

SLMs – Spatial Light Modulation

n – Director (unitary vector)

P – Cholesteric pitch

AGU – Anydroglucopyranose

DP – Degree of Polymerization

PEG – Polyethyleneglycol

PVA – Polyvynil alcohol

Gly – Glycine

Pro – Proline

Hyp – Hydroxyproline

PCL – Polycaprolactone

PC – Phosphorylcholine

SBMA – Sulfobetaine Methacrylate

CBMA – Carboxybetaine Methacrylate

HDNF – Human Dermal Neonatal Fibroblasts

FBS – Fetal Bovine Serum

DMEM – Dulbecco's Modified Eagle Medium

EDTA – Ethylenediamine Tetracetic Acid

PBS – Phosphate-buffered Saline

DF-1 – Dermal Fibroblast Culture Medium

FTIR – Fourier Transform infra-red spectroscopy

ATR – Attenuated Total Reflectance

SEM – Scanning Electron Microscopy

CCD – Charged Couple Device

EDS – Energy Dispersive Spectroscopy

TEM – Transmission Electron Microscopy

POM – Polarized Optical Microscopy

EKA – Electro Kinetic Analysis

LVR – Linear Viscoelastic Region

MCC – Microcrystalline Cellulose

FWHM – Full width at half-maximum

BNC – Bacterial Nanocellulose

Chapter I – Introduction

1. Liquid Crystals:

1.1. Liquid Crystals: Definition and Characterization

Liquid crystals (LCs) are widely used in different fields such as tissue engineering [2], drug delivery [6] and electronics, for example as a component in a TV screen. [7] LCs are well known for their intermediate state between isotropic liquids and crystalline solids with a three dimensional structure (figure 1.1). Thus, their chemistry and physics has been profoundly studied throughout the years, having a rapid advance after 1960. The discovery of the liquid crystalline state was made by the botanist Freiderich Reinitzer in 1888. Reinitzer described a colour arise when melting cholesteric acetate and cholesteric benzoate. In addition, two melting points of the cholesteric benzoate were registered and for the first time the term liquid crystal was applied. [8] In 1904, Otto Lehmann, a German physicist, with whom Reinitzer corresponded, proceeded with the study of this state of matter and later associated these properties with some biological samples. From 1960 with the application of liquid crystals in televisions and other electronic devices, numerous progresses were made in this field. [9]

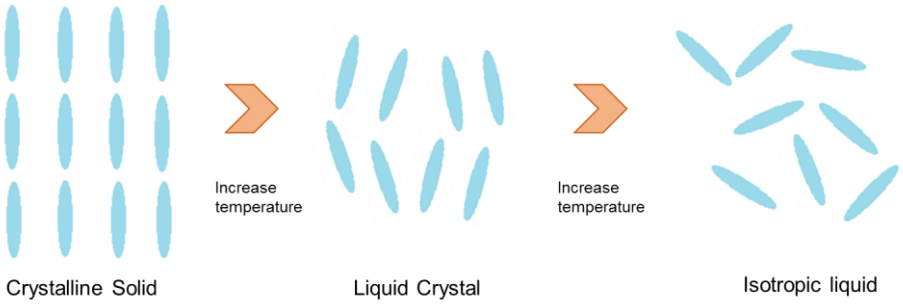

Figure 1.1 – Schematic of the thermal transitions regarding the liquid crystalline state.

There are two major categories of liquid crystals: thermotropic and lyotropic. Thermotropic liquid crystals are formed with anisotropic molecules that self-assemble in arranged structures according to the temperature. This mesophase exists between full alignment of particles (crystalline state) and the isotropic state, which occurs at a higher temperature. In another words, thermotropic LCs result from heating a crystalline solid or cooling an isotropic liquid reaching a thermodynamic equilibrium. [8] They are also formed by applying certain conditions of pressure. [10] Lyotropic LCs are formed with the addition of a solvent to one or a mixture of compounds and depends on the concentration of the mesogen (a compound that in certain conditions of

temperature, pressure or concentration is a precursor of a mesophase or a liquid crystalline phase) and also on the temperature and pressure conditions. [8]

Thermotropic LCs integrate rod-like, disk-like or banana-shaped molecules that arrange in three different phases: nematic, cholesteric and smectic. [11] The most common liquid- crystal phase is the nematic, identified by a long range orientational order with the direction of a dimensionless vector **n**, called director. In the nematic phase molecules tend to align in the same direction as the long axis, that is, in the same direction as the director with no specific positional order. A cholesteric phase or chiral nematic phase is formed by optically active organic compounds (chiral molecules), a mixture of different types of these compounds or a mixture of optically active compounds with nematic liquid crystals. A chiral molecule is one that cannot be superposed to its mirror image. [9] Cholesteric liquid crystals have a helical twist: the director vector, **n**, pursues a helical form. The distance for a 360º turn is denominated pitch. Nematic LCs have an infinite pitch and by chemical or mechanical processes they can be converted to the cholesteric liquid crystalline phase. In the figure 1.2 is represented a three dimensional scheme of this phase, where the molecules are represented by parallel lines and rotate in each level by a constant and small angle. When the rotation reaches 180º, half pitch is defined. This model is called plywood model. [12]

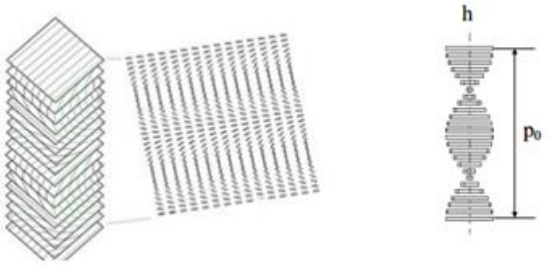

Figure 1.2 – Three dimensional representation of the cholesteric liquid crystalline phase (plywood model). On each level the molecular arrangement is represented by parallel lines and they rotate continuously in a small and constant angle. P0 – pitch. [13]

Chiral nematic LCs have unique optical properties. When a perpendicular beam of light with a wavelength much smaller than the pitch reaches the LC, it is broken in two: one perpendicular and other parallel to the alignment axis – this phenomenon is called birefringence. When the pitch is reduced, the beam is converted into a circular polarized wave and the LC shows optical activity. This optical property is dependent on the wavelength of the irradiation beam and on the dielectric constant of the LC material. [9]

Smectic liquid crystals are arranged in layers and have long range organizational order, that is, the long axis is parallel to each layer. Depending on the molecular order in a layer, there are two different subtypes of smectic LCs: unstructured and structured. Structured LCs have long range order in the molecules arrangement and form a two dimensional lattice. In contrast, in unstructured LCs the molecules in the layer do not have any specific order. [9]

In figure 1.3 are represented three phases of the thermotropic liquid crystals:

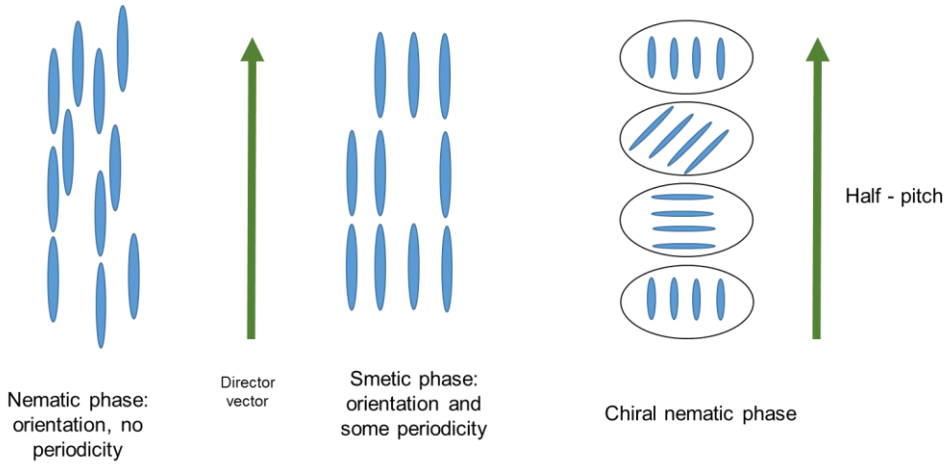

Figure 1.3 – Schematic of three phases of the thermotropic liquid crystals: Nematic, Smectic and Cholesteric. Adapted from [9].

Usually lyotropic liquid crystals are formed by an amphiphilic molecule and a solvent [11] at a given temperature and relative concentrations. These molecules self-aggregate in a minimum energy supramolecular structure and the most prevalent form is the lamellar, where the double layers are parallel to each other and are separated by the solvent. Other lyotropic arrangements consist in cubic, hexagonal, micellar and gel. [9] The most common phase in lyotropic liquid crystals is the chiral nematic but achiral phase like smectic and nematic are also observed. [14]

1.2. Liquid Crystals in biology:

Liquid crystallinity is found in numerous biological molecules such as, proteins, carbohydrates, fats, acid nuclei and virus. Furthermore, the liquid crystalline phase is proved to be involved in the beginning of the formation of biological molecules and it is considered an important step of the differentiation process of cells and tissue [1]; LCs are also responsible for the morphogenesis of tissue, tendons and ligaments. [15] For instance, it was observed that procollagen had pre-cholesteric phases that induced the structure of some animal tissues, which are anisotropic and present a fibrillary structure. [16][17]

The double helix structure of DNA and RNA show a chiral nematic LC phase of these organic compounds. Proteins exhibit the same behaviour and both form rods that combine into hexagonal structures. The phospholipid bilayer also has a lyotropic liquid crystalline conformation with a lamellar phase, which indicates a smectic phase [18]; lipid esters and carotenoids in contact with water also exhibit liquid crystalline phases. [9] Myelin is also a phospholipid membrane with LC behaviour; however, it is made of several concentric stacked bilayers. [14][18] Some proteins, like haemoglobin in water, is packed in layers, forming a nematic LC phase. [9] The polysaccharides chitin and cellulose, the first, present in carapace of crustaceans and the second in plant cell walls have a plywood structure and consequently a chiral nematic order. [18][19]

Cellulose, particularly nanocrystalline cellulose (NCC), in aqueous suspensions, shows liquid crystalline behaviour, being a lyotropic LC, and has a chiral nematic arrangement. [19] On the other hand, collagen molecules are triple helical, thus, also chiral nematic and posteriorly organize into cross-striated fibrils and in a three dimensional network. [20] This type of assembly is present in compact bones, connective tissues and cornea. In human compact bone, collagen type I has arced textures due to the superposition of different molecules orientations at the section plane. [17] In cuticles, the collagen molecules form concentric circles. [12]

In table 1.1 a summary of some biological liquid crystals and its corresponding liquid crystalline phases is presented:

Table 1.1 – Biological liquid crystals and type of LC phase:

Biologic liquid crystal	Liquid Crystalline Phase
DNA [9]	Chiral Nematic
RNA [9]	Chiral Nematic
Proteins [9]	Chiral Nematic
Phospholipid bilayer [18]	Smectic
Myelin [14]	-
Haemoglobin [9]	Nematic
Chitin [18] [19]	Chiral Nematic
Cellulose [18] [19]	Chiral Nematic
Collagen [20]	Chiral Nematic

Liquid crystalline behaviour enhances some properties of the biological materials such as elasticity, resistance to load and stress. [21] This characteristic also allows efficient packing and self-assembly of plywood structure and sensor/actuator abilities. [22]

1.3. Liquid crystals in biomedical applications:

Liquid crystals are widely used in biomedical applications due to their unique properties such as birefringence and the ability to change their conformation in the presence of an external field as light, voltage and heat. In some external conditions, such as in the presence of chemical or biological substances or pH variations, LCs can also change their conformation. Furthermore, LCs have an affordable cost and are resistant to stress and elongation. The possibility to mimic biological arrangements and to react to electromechanical stimulus, taking part of artificial structures such as muscles and bones, enables a new type of prosthesis that can execute complex tasks.

Chiral nematic printed LC films are being used for temperature and humidity actuators. These LCs are implemented as power generators, smart textiles, artificial muscles, and sensors. The pitch and wettability of these LC superficies change with the radiation beam (temperature). [23]

Another employment of LCs in this field includes: liquid-crystal tunable filters (LCTFs) and spatial light modulators (SLMs). LCTFs are used in spectroscopy, acquiring the spectral signature of a cell, tissue or a biological particle. As an example, the spectral signature of the haemoglobin, present in the blood vessels of human conjunctiva, can be detected by the LCTFs and used to diagnose anaemia by measuring the haemoglobin levels. Allied with optical fibres this technique also allows endoscopic diagnosis. SLMs are used in DNA manipulation and in the investigation of cellular behaviour as well as in *in vitro* fertilization practices. These devices brought more phase contrast and led to advances in scanning microscopy. LCs are also used to produce, on a larger scale, lasers with higher optical range and optical power that, with further research, will bring advantages in the biomedical field. LCs nematic droplets can function as lenses with a focal length that can be modulated with an electric field. They can substitute bifocal eyeglasses by switching to near or far vision with the electric stimulus. [11]

A variety of molecules such as antigens, are added to liquid crystals to form chemical and biological sensors. When a surface interaction occurs in the LC, its conformation changes, forming a simple and rapid sensor that doesn´t need biological markers or any kind of energy to function. [11] On the other hand, it was reported that an endotoxin aggregated to LC droplets' defects, is able to change the droplet´s conformation. [24] Brake et al. observed an alteration of the alignment in LCs, when phospholipids are added to the liquid crystal aqueous interface. [25]

In the field of tissue engineering, hydrogels and silicon elastomers with LC properties were applied to the study of cell behaviour. Liquid crystals were added to a cell culture of mammalian cells and it was observed cell proliferation, proving the non-toxicity of certain LCs to this type of cells. [2] Liquid crystalline collagen was reported to align fibroblasts in a parallel direction to the collagen matrix direction, supporting the role of LCs in tissue formation. [26] It was also used to understand the influence of the matrix architecture on cell behaviour. [3] Collagen fibrils, hydrated with a liquid crystalline phase, were shown to successfully grow an amount of fibroblasts, close to the number of fibroblasts presented in the connective tissue, representing an enormous breakthrough in tissue regeneration and in the production of new materials similar to skeletal tissue [27], corneal and in the regrowth of peripheral nerve axons. [28] Genetically engineered liquid crystalline films of virus M13, coated with peptides, are proved to aid in the growth of nerve cells. [29]

Lyotropic liquid crystals, such as GMO/PT–propyleneglycol–water systems, are also being investigating to be used as drug delivery systems in cancer treatments by photodynamic therapy. [30] These materials have non-toxic, biodegradable and bioadhesive properties and are

able to encapsulate, in its lyotropic layer, substances of low and high molecular weight such as, chemical drugs, proteins, peptides and nucleic acids for drug delivery systems. [6]

2. Cellulose and collagen: two liquid crystalline biomaterials:

Cellulose is the most common and important natural organic polymer and is a long-chain polysaccharide with repeating unites of D-anhydroglucopyranose linked by a β-1,4 glycosidic bond. It´s molecular structure is represented in figure 1.4. The main properties of cellulose are hydrophilicity, chirality, degradability and the formation of supramolecular assemblies by hydrogen bonds, due to the presence of three reactive hydroxyl groups. [31] Cellulose can be found in plants, some bacteria, algae and fungi. [32]

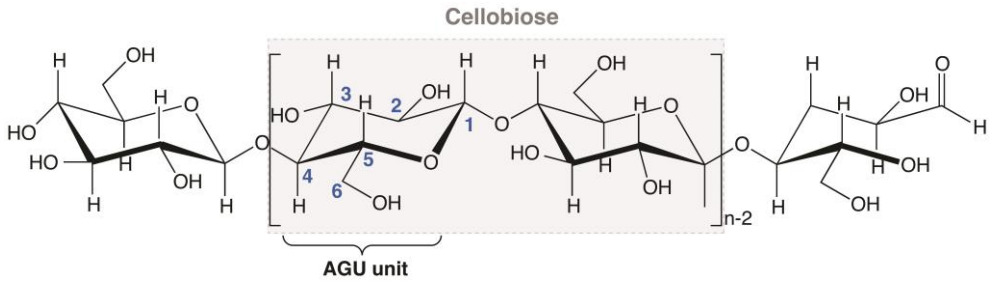

Figure 1.4 – Molecular structure of cellulose representing the cellobiose unit as a repeating unit, showing the non-reducing (left) and reducing (right) end-groups. This structure also shows that the repeated anydroglucopyranose units (AGU) are rotated of 180º with respect to each other, due to β- linkage constrains (n=DP, degree of polymerization)**.**

Improvement of the knowledge of the reactivity and structural features of cellulose has motivated the search for new types of cellulose-based materials - ethers, esters and nanocellulose.

On the basis of its functions, dimensions and preparation methods three categories of nanocellulose can be considered: microfibrillated cellulose, bacterial nanocellulose and nanocrystalline cellulose. [33]

Nanocrystalline cellulose (NCC) nanoparticles are rigid rod-like crystals, with 5-70 nm of width and 100 or more nm of length, obtained by acid hydrolysis of cellulose fibres. NCC has a high surface area, which increases its reactivity, possess less toxicity and presents enhanced mechanical properties when used in a composite mixture. Besides, NCC is bio- and hemo-compatible and has unique optical properties. In an aqueous suspension, NCC shows an isotropic phase that is converted in a chiral nematic liquid crystalline phase when the NCC concentration

rises above a critical point, observed by the appearance of birefringence and a characteristic fingerprint texture. [34] NCC can also show a parallel alignment when exposed to a magnetic field. [35] Nanocrystalline cellulose has been studied for various tissue engineering applications in the past few years. NCC can be used as scaffolds, films, porous sponges and as hydrogels reinforcement agents, increasing their mechanical properties and biocompatibility. [32] Burt et al. studied the ability of NCC to bind to water soluble antibiotics and cationic NCC to bind to non-ionized hydrophobic anticancer agents, proving that these systems are good drug carriers either in the form of films, hydrogels or microspheres. In blood vessel replacements, NCC also improved the mechanical properties of implant matrices of collagen, gelatin, alginate, chitosan, cotton gauze, polyethylene glycol (PEG) and polyvinyl alcohol (PVA). [36] Yang et al. produced injectable hydrogels of carboxymethyl cellulose and dextran reinforced with cellulose nanocrystals and aldehyde-functionalized NCC, as a chemical cross-linking agent. These hydrogels, with high dimensional stability in swelling experiments and improved mechanical properties, exhibit non-significant cytotoxicity when in contact with 3T3 fibroblast, which opens its use to several biomedical applications such as drug delivery systems or tissue engineering matrices. [37]

Collagen is the most common protein present in the human body and is the main structural element of tissue, skin, bone and cartilage. It is formed by three filaments of polypeptides combined in a left-handed triple helix with 300 nm long and 1.5 nm of diameter. Collagen is characterized by Gly–Pro–Hyp–Gly–X–Y sequences where Gly is glycine; Pro is proline, Hyp is hydroxyproline, X and Y are amino acids, linked by hydrogen bonds between –CO and –NH groups, and by covalent bonds. [26] Its precursor is procollagen, a molecule with N and –C terminals groups that are posteriorly removed to form collagen. [16]

There are 19 types of collagen known. Type I collagen forms most of the extra cellular matrix proteins of dense connective tissue. The hierarchical organisation of these fibrils increases the elasticity of skin, the resistance to stress or shear in tendons, the load in bone and transparency of the cornea. *In vitro* research proved the existence of liquid crystalline chiral nematic phase of type I collagen with a long-range helical order. [20] A major interest in collagen in tissue engineering field has grown due to collagen's biocompatibility, biodegradability, low immunogenicity and toxicity as well as good cell adhesion properties. [27]

Collagen is used in drug delivery systems in films, such as collagen shields in ophthalmology for surface lubrication [38], and as a sponge, to delivery certain drugs through the eye [39] and for wounds and bruises. It is additionally applied as a homeostatic agent. In tissue engineering, collagen matrices can be used for bone regeneration and cell growth however the growth of extracellular matrices takes a long time. [40] Stopak et al. verified that collagen gels, which were formed shortly after the injection of collagen, in developing chick limb buds, rearrange with the limb tissue and are able to form parts of tendon, perichondria, perineuria, and other

structures. [41] Kofidis et al., showed, with *in vitro studies,* that projected collagen devices colonized with cardyomiocites with continuous and synchronized contractions are close to be suitable to repair cardiac tissue. [42] Collagen type I alone is used as bone substitutes and tissue grafts due to its osteoconductive activity. Furthermore, mixtures of hydroxyapatite with demineralized bone collagen are employed as bone grafts materials. [43]

3. Physical and chemical gels:

Gels are a viscoelastic soft material, which combines a solvent and an elastic cross-linking network. The solvent is captured and adhered in the solid arrangement. If gels are formed by strong chemical bonds they are thermally irreversible and they cannot be disassembled. On the other hand, gels formed by weak and non-covalent interactions can be dismantled. [44] A chemical gel is a polymer 3D network chemically bounded to each other by covalent bonds. Physical gels are 3D assembled structures of fibrous low molecular weight compounds. The interactions between molecules to form fibrous structures are hydrogen bonds, π-π and donor-acceptor interactions. [45]

Liquid crystalline chemical gels are formed by in situ polymerization of monomers that can or cannot be liquid crystals with reactive groups in inert liquid crystal solutions. LC physical gels arise from the self-assembly of a fibrous low molecular weight structure (gelator) that imprisons the liquid crystal. The transition of sol-gel of the gelator and the isotropic-anisotropic transition of the liquid crystal occur in the gel formation process. [45] Figure 1.5 shows the illustration of physical and chemical gels as well as of the physical and chemical liquid crystal gels.

Liquid crystalline gels can be thermoreversible and have phase transitions: isotropic liquid-isotropic gel and isotropic gel-liquid crystalline gel that are independent of each other but dependent of the temperature. [45]

In the opto-electronic field, liquid crystalline physical gels are being studied due to their ability to change from a light scattering state to a light transmission state with an applied voltage. These LC gels, formed by oligo (amino acid) gelators, are a great advance for electro optical displays. [46] Bistable nematic liquid crystal gels with self-assembled fibers, which are thermoreversibles can be applied to the manufacturing of rewritable memory. Light can also change the LC gel conformation and can be applied to produce electrically switchable diffracting gratings. [45]

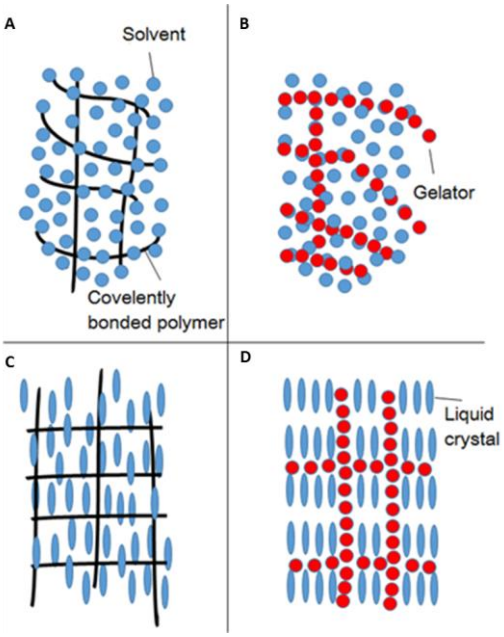

Figure 1.5 – Illustration of: a) chemical gels; b) physical gels; c) Liquid-crystalline chemical gel; d) Liquid-crystalline physical gel. Adapted from [45].

3.1. Hydrogels:

Hydrogels are hydrophilic polymer networks that are capable of swell and adsorb water in a quantity higher than its weight. They present a physical structure similar to a biologic cellular matrix and can be used to modulate and study the cellular behaviour and tissue morphogenesis. Furthermore, hydrogels are suitable for a wide range of biomedical applications: 3D matrices for tissue engineering, drug delivery systems, injectable fillers for minimally invasive surgeries and composite biomaterials. [47]

Physical and chemical hydrogels are distinguished by the definition applied to gels (see physical and chemical gels). When the variation of physical condition such as pH, temperature, ionic strength or application of external forces occurs, the hydrogel may disintegrate and dissolve. [48]

Peppas et al. stated that hydrogels are obtained by swelling cross-linked structures in water. The different processes to form a hydrogel are: chemical cross-linking, photopolymerization and irradiative cross-linking. Chemical cross-linking can cover bulk polymerization, suspension polymerization and cross-linking. Photopolymerization is mostly used with UV light, which activates certain functional groups to form covalent bonds with radicals. [44] At last, irradiative cross-linking consists in generating radicals by ionizing radiation; these radicals are not bonded to chains and recombine to form crosslink junctions. [49] Also physical interactions like crystalline formations, entanglements and electrostatic forces lead to hydrogel formation. [50]

Cellulose is able to absorb large quantities of water, mainly dependent on its crystalline and amorphous regions, total surface area and pore volume, which makes it suitable for use in

hydrogels. [51] NCC, which have higher degree of crystallinity, surface area and pore volume are used to produce hydrogels and are gelated with, for instance, the addiction of certain polysaccharides. [52] Others examples of NCC hydrogels can be found in the literature. For example, the NCC are gelated with polymers, as polyethylene glycol and poly(methyl vinyl ether-co-maleic) acid, to produce hydrogels with enhanced physical properties. [50] In another research, NCC were incorporated into hydrogels based on cyclodextrin/polymer inclusion and these hydrogels, can possibly be used as a controlled drug delivery vehicle. [34]

Collagen hydrogels are easy to handle, although they present weak mechanical properties and non-controllable swelling. Concentrated collagen hydrogels were studied to surpass these disadvantages and it was shown that the hydrolysis of the gel was retarded comparing to collagen gels. Furthermore, they favour cell growth and do not contract drastically, making them suitable for dermal substitution. [53]

Elastomeric hydrogels are being developed by Betre et al., for biomedical applications due to its elasticity similar to skin, blood vessels, lungs and muscle. These gels are prepared from a mixture of α-elastin with polycaprolactone (PCL) that stimulate chondrocyte adhesion and proliferation. Chondrocytes were implanted in a collagen, alginate and K-elastin composite and the cartilage formation was observed. [54][55]

4. Polyvynil Alcohol (PVA):

PVA is a synthetic polymer that is widely used due to its biocompatibility and ability to produce macroporous hydrogels suitable for tissue engineering [56] and drug delivery systems [57]. PVA has good elastic and mechanical properties, such as tensile strength, and it can be dissolved in water. [57] Hydrogels of PVA and NCC were reported by Abitbol et al. and are formed by cyclic freezing and thawing. This method allows the formation of hydrogels with good stability at room temperature and prevents toxicity derived from PVA. These hydrogels present a similar water content of the biological tissues, have good elasticity and are thermoreversible at 50°C. [58] The crystallites formed in the freeze cycles act as a cross-linking agent forming a hydrogel with a pure crystalline network.

PVA is a polymer widely used in biomedical applications. Having this in mind gels of NCC/PVA were explored as a fluorescence biosensor that can be employed in wound diagnosis. [59] Gonzalez et al. showed a potential use of hydrogels with NCC/PVA for wound dressing. [60]

5. Cell adhesion mechanisms:

5.1. Protein adsorption:

To occur cell adhesion, firstly there has to exist protein adsorption by the biomaterial's surface. A monolayer of proteins is able to adhere on the biomaterial shortly after the first contact protein-biomaterial. This monolayer is fundamentally responsible for cell adhesion and for a positive response of the body to an implanted biomaterial or, in case of scaffolds, cell proliferation. [49]

The cell membrane possesses integrins, which are receptors that bind to specific protein types. The proteins that enhance cell adhesion differ from cell line to cell line. As an example, fibronectin improves cell adhesion in fibroblasts but the contrary is shown with endothelial cells. Albumin is also known to decrease cell adhesion in fibroblasts and vitronectin enhances the adhesion of endothelial cells. Protein absorption is a competitive process and thus, concentration of different proteins should be taken into account in the culture medium. [49]

The proteins' size, charge, structure stability and unfolding rate are some of the properties that influence the interaction with the material's surface. For instance larger proteins, or proteins with a higher unfolding rate and even less stable proteins have more binding sites and thus lead to a more efficiently cell adhesion. Proteins near the isoelectric point, (the pH at which the molecule exhibits zero charge), have a better cell adhesion rate. [61]

Several studies also show that hydrophobic surfaces can more easily irreversibly bound to proteins due to the protein unfolding on the surface. At low ionic strengths, cationic proteins bind to anionic surfaces, as well as anionic proteins bind to cationic surfaces. These protein preferences are due to the ion-ion coulombic forces. [62]

The cell adhesion process is also influenced by surfaces with textures, which extends its surface area, heterogeneity and chemical composition of the surface. [61]

In contrast, the osmotic repulsion, dehydration between protein-surface, chain compression and protein hydrophobic exposure opposes to protein bounding. Van der Waals forces and desorption of water molecules also favour the protein-surface adhesion. [49]

In conclusion, protein adsorption is a complex mechanism and it is still being studied. The main reason for a biomaterial resist to protein adsorption relies on the retention of bound water by the surface molecules.

5.2. Non-fouling biomaterials:

Non-fouling biomaterials do not have a surface suitable for a good protein and/or cell adhesion. Strong protein adsorption can also inhibit cell adhesion to the material. Although these materials cannot be used for tissue engineering purposes, they do have diverse biomedical

applications such as implanted devices, urinary catheters, diagnostic assays, biosensors, affinity separations, microchannel flow devices, intravenous syringes and tubing. In a non-biomedical field non-fouling materials are used as biofouling-resistant heat exchangers and ship bottoms. [49] They are also used in *in vivo* nanoparticle-based diagnostics and microarrays. Currently, few non-fouling materials can be used in biomedical applications without suffering any kind of degradation such as PEG, phosphorylcholine (PC) and sulfobetaine methacrylate (SBMA) and carboxybetaine methacrylate (CBMA). [63]

5.3. Improvement of cell adhesion in non-fouling materials:

For tissue engineering purposes, good protein adhesion to the materials or surfaces are essential. Hence, several physical (etching, roughening and photolithographic techniques) [64] and chemical (cross-linking of polyelectrolyte multilayer films [64], addition of RGD peptide [65], oxidation, fluorination and silanization [49]) methods have been developed to improve cell adhesion in biomaterials.

6. Fibroblasts: a cell culture perspective.

6.1. Fibroblasts:

Fibroblasts are mesenchymal cells responsible by production of growth factors and the main components of the extracellular matrix such as, interstitial collagens, proteoglycans, glycoproteins, cytokines, and proteases. [66] They are part of the connective tissue family, which also includes cartilage (chondrocyte) and bone (osteoblast and osteocyte) cells. They are found dispersed through the connective tissue of an organ and repair the human tissue by migrating to the wounded site and then excrete the extracellular matrix. [67]

Morphologically, fibroblasts have a spindle shaped flattened conformation [68] with an oval nucleus. When adhesion to fibbers occurs, they form a three dimensional network and become embedded within the extracellular matrix. Fibroblasts isolated from either different or equal sites, show heterogeneous phenotypes [69] and currently there are no specific markers for fibroblasts, difficulting their study. [70] The origin of this cell line is still being studied. [71] Some type of fibroblasts can differentiate into other cells of its connective tissue family and in adipocytes, in specific conditions of the extracellular matrix, growth factors, cell shape and hormones, which is represented in figure 1.6. [67]

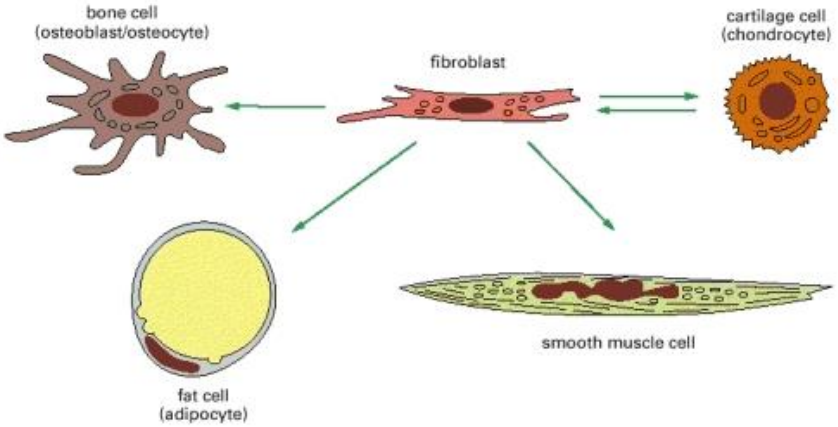

Figure 1.6 – Illustration of the connective tissue cell family. The fibroblasts can in certain conditions of extracellular matrix, growth factors, cell shape and hormones differentiate in other cells of the connective tissue family. Adapted from [67].

Recent studies also showed that fibroblasts have an important role in the angiogenesis process. [72] Furthermore, researches concluded that fibroblasts can differentiate into endothelial cells as well as, endothelial cells can differentiate into fibroblasts. This recent discovery opened new possibilities for in situ tissue repair. [73]

6.2. Fibroblasts in tissue engineering:

In 1975, the first techniques to culture fibroblasts were established by Rheinwald and Green with 3T3 murine fibroblasts. Fibroblasts are vastly used in cell culture on account of its individual behaviour (they do not form clusters) and the ability to adhere to plastic surfaces. In specific, dermal fibroblasts can be easily expanded from a small skin sample without refined purification methods, by enzymatic degradation or explant culture. For fibroblasts to grow there is no need for growth factors and one culture expand rapidly (24-72 hours) in the presence of serum. [74]

As previously mentioned, fibroblasts are able to migrate to injury sites and to differentiate into another connective tissue lineage cells, including bone, cartilage and adipose cells. Based on these unique properties, numerous studies were carried out until today focusing in fibroblasts and their potential in tissue engineering.

Fibroblasts are being used to repair ligaments [75], skin defects such as acne scars and rhytids [76], and when used in a collagen matrix for the treatment of burns. [77] Parmer et al., also combined collagen matrix with fibroblasts to reconstruct epithelial-stroma interactions, helping the growth of human mammary epithelium in mice. [78] In another study the authors showed that a derived dermal substitute with human fibroblasts successfully improved the healing of diabetic foot ulcers. [79] Also, clinical trials indicated that spray formulations of allogeneic neonatal keratinocytes and fibroblasts aid the treatment of chronic venous leg ulcers. [80] Syedain et al.,

conducted investigations regarding implantable arterial grafts obtained by entrapment of human dermal fibroblasts in fibrin. Their team created grafts with similar aorta's retention strength. [81] Co-culture of bone marrow fibroblasts and endothelial cells in polycaprolactone substrates showed good results for bone tissue engineering. [82]

6.3. Fibroblasts and liquid crystalline structures:

Fibroblasts were already used with liquid crystalline materials, demonstrating the importance of the liquid crystals in new therapies based in tissue engineering techniques.

Fibroblasts were successfully cell cultured in collagen type I gels with liquid crystalline textures. Furthermore, after one month of incubation, the number of fibroblasts is approximately the same as estimated in the connective tissue. [27] Kirkwood et al., as previously described in these chapter, observed the directional growth of fibroblasts according to the chiral nematic phase of the type I collagen gels, opening new perspectives in recreating the original connective tissue textures *in vitro*, for posterior tissue engineering purposes. [26]

Chung et al., produced M13 bacteriophages liquid crystalline films and fibers for directional growth and successfully encapsulated fibroblasts. The results of these experiments were the guidance of the fibroblasts growth. [83]

Chapter II - Materials and Methods

1. Nanocrystalline Cellulose gels:

1.1. Materials:

All materials were used as received unless stated otherwise. Microcrystalline cellulose, Avicel® PH-1010, 50 μm particle size, was purchased from Sigma-Aldrich. Sulfuric Acid (95-97%, p.a) was used in the acid hydrolysis reaction of cellulose and was purchased from Merck. Glycerol (pharmaceutical grade) was purchased from Laborspirit and polyvinyl alcohol (95%, M_w=95000 g/mol) was purchased from Acros Organics. Dilutions were always performed using ultrapure water from a Millipore Elix Advantage 3 purification system. Collagen, from bovine Achilles tendon, was purchased from Sigma-Aldrich (St. Louis – USA). Glacial acetic acid (99.7%, p.a.) and ammonia (25%, p.a.) were purchased from Panreac. Yellow food dye was supplied by Globo.

Cryopreserved Human Neonatal Dermal fibroblasts (HNDF) were purchased from ZenBio. Modified Eagle Medium (DMEM), with 10% fetal bovine serum (FBS), the essential culture medium was acquired from Dulbecco's. The solution of 0.25% trypsin/2.21 mM EDTA (ethylenediamine tetraacetic acid) were purchased from Gibco. FBS was supplied by EC approved origin, LDA. Resazurin (resazurin sodium salt at 0.1 mg/mL) was purchased from Sigma-Aldrich. Phosphate-buffered saline (PBS) was prepared at INEB by a laboratory technician.

1.2. Acid hydrolysis of cellulose:

To produce nanocrystalline cellulose (NCC), acid hydrolysis of microcrystalline cellulose was performed based on the works of Gray group [84][85] and Orts et al. [86] with minor adaptations. 10g of microcrystalline cellulose were hydrolysed in a mixture of 87.50 mL of sulphuric acid and 84 mL of distilled water at 45ºC, under vigorous magnetic stirring. Three reaction times were set: 40 minutes, 70 minutes and 130 minutes. After the hydrolysis time was concluded, the suspension was added to a 3L beaker with 10 fold of ultrapure water. The suspension was placed at rest for 16 hours. After this time, the suspension presented two phases: the acid in the top and the NCC/MCC deposited at the bottom of the beaker. The acid was retrieved with a pipette and the NCC suspension was washed with ultrapure water by centrifugation, at 12000 rpm for 30 minutes. This washing process was repeated until a pH of 3.4 was reached, normally attained after 2-3 full working days. A Thermo Scientific Heraeus Multifuge X1R was used for the centrifugation. After this process, the remaining NCC suspension was

centrifuge at 14000 rpm for an hour in order to concentrate the suspension. The resulting suspension was placed in a Spectra/Por® 4 cellulose membrane (from Spectrum), with a cut-off of 12-14 KDa, and dialyzed against ultrapure water until a constant pH value was achieved (normally ~5.5 to 6.0). [84]

The amount of NCC in a given suspension was controlled by gravimetric study (10 measurements). In this procedure small quantities of NCC suspension were dry, on an oven at 60 ºC, until constant weight. Higher contents of NCC in a suspension could be obtained by centrifugation. All suspensions were sonicated, with an ultrasonic processor UP400s (400W, 24kHz, Hieslcher Ultrasonics GmbH), prior to use.

Pictures of NCC suspension's birefringence, observed by placing the suspension vial between two cross polarizers sheets (from Edmund Optics), were acquire by using a Casio EX-F1 Exilim Pro camera. A light source was used behind the vial.

1.3. NCC/glycerol gel formation:

Gelation was performed according to Dorris et al. procedure. [87] Typically glycerol was added to the NCC suspension and the mixture was stirred vigorously for about 30 minutes or until a homogeneous suspension was achieved. Then the mixture was placed in an oven at 60ºC until almost all the water is evaporated. The evaporation of the water was controlled by gravimetric method, this is, until constant weight. The NCC/glycerol ratio was adjusted by changing the amount of glycerol added to the NCC suspension. For instance, to obtain a gel with 5% (w/w) of NCC, to 5g of 2.5% (w/w) NCC suspension 2.5g of glycerol was added and this ratio was used for further concentration calculations. Gels with different NCC contents were obtained and are summarized in table 2.1.

Table 2.1 – Amount of NCC and glycerol used in the NCC/glycerol gels preparation. Final NCC content in the gels (value rounded to the integer).

Gel	% NCC in H_2O suspension (w/w)	m (NCC/H_2O suspension) (g)	m glycerol (g)	Final NCC % in the gel (w/w)
A	2.124	2.5	1.593	3
B	2.124	2.5	1.062	5
C	2.124	2.5	0.490	10
D	2.124	2.5	0.245	18
NCCs40' NCCs70' NCCs130'	2.124	2.5	0.708	7

To distinguish the gels with different hydrolysis times, the following nomenclature will be used through the study of the NCC/glycerol gels with 7% (w/w) of NCC in their composition:

- NCCs40': gels containing NCC with 40' sulphuric acid hydrolysis time;
- NCCs70': gels with 70' NCC sulphuric acid hydrolysis time;
- NCCs130': gels with 130' NCC sulphuric acid hydrolysis time.

The remaining concentrations of NCC in the NCC/glycerol gels do not follow any specific nomenclature.

1.4. NCC/PVA gel formation:

Gels of NCC and PVA were prepared according to Abitbol et al. by cyclic freezing and thawing. PVA was dissolved in a ratio of 15g of PVA to 100g of water. After complete dissolution, the aqueous suspension of NCC was added to this mixture and left under stirring for 24 hours. The resultant suspension was placed in an oven at 90ºC during 6 hours proceeded by 24 hours of stirring at room temperature. 5 freeze-thawing cycles were performed to the sample. The freeze cycle lasted 18 hours at -18 ºC and the thawing cycle 4 hours at room temperature. To study the most viable gel for cell culture, gels with different NCC/PVA ratios (table 2.2) were prepared. [58]

Table 2.2 – Amount of NCC and PVA used in the NCC/PVA gels preparation. Final NCC content in the gels.

Gel	% NCC in H_2O suspension (w/w)	m (NCC/H_2O suspension) (g)	m PVA (g)	m H_2O (g)	NCC % of dry weight of PVA
A	2.124	2.833	0.604	1.256	10
B	2.124	0.304	1.000	6.370	0.65
C	2.124	2.354	1.038	4.617	4.85

2. Collagen gels formation:

2.1. Gel formation:

The preparation of collagen gels followed the work presented by Giraud-Guille et al., Typically collagen was dissolved in a 0.5M solution of acetic acid, in order to form a 5mg/mL solution. Rapid stirring, during 72 hours at 4ºC, was required for full dissolution of collagen. The solution was then sonicated to destroy collagen agglomerates. Solvent evaporation was obtained with reduced pressure (with an Edwards RV5 vacuum pump) until a 40 mg/mL concentration was reached. The sample was then sonicated to obtain a homogenous solution for a better distribution in a 96 well plate. The well plate was placed in an ammonia chamber for gel formation for a month. [3]

3. Characterization of the Nanocrystalline cellulose and its gels:

3.1. Fourier Transform infra-red spectroscopy (FTIR):

Dry samples of NCC, as thin films, were analyzed by FTIR. Thin films of NCC suspensions were casted onto polystyrene molds by solvent casting methods. NCC films were analyzed at Cenimat|I3N by a FTIR Thermo Nicolet 6700 spectrometer coupled with an attenuated total reflectance (ATR) sampling accessory (Smart iTR). ATR-FTIR spectra were recorder with an incident angle of 45º, from 4000-600 cm^{-1}, with 4 cm^{-1} resolution, 32 scans at room temperature.

ATR-FTIR spectra of the NCC gels, before and after exposure to cell culture medium, were acquired at INEB with a Perkin-Elmer 2000 system 2000 XR-analysis.

3.2. X-Ray Diffraction:

The structural analysis of NCC and microcrystalline cellulose was achieved by collecting X-Ray Diffraction patterns. This was done using a XRD PANalytical (model X'Pert Pro) in Bragg–Brentano geometry with Cu Kα line radiation (λ=1.5406 Å) at 45 kV and 40 mA, the instrument being equipped with an X'Celerator detector. The XRD patterns were collected with a scanning step of 0.0334° over the angular 2θ range 10°–40°, with a total acquisition time of 4 min. To analyze the diffractograms, specific software (OriginPro 8) was used that allows the characterization of the peak parameters such as position, intensity, width and shape.

3.3. Scanning Electron Microscopy (SEM):

Scanning electron microscopy (SEM) uses a high energy electron beam to target a sample. The electrons carry a kinetic energy, which is transferred to the sample's surface due to the deceleration of the electrons, emitting secondary electrons. These secondary electrons generate a current that is measured by charged coupled device (CCD) screens, originating the SEM image. A SEM image is a representation of the specimen topology. On the other hand, backscattered electrons – primary electrons that are dispersed after the collision with the sample, provide a chemical analysis of the material – EDS (energy dispersive spectroscopy). [61] A scheme of a scanning electron microscope is represented in figure 2.1:

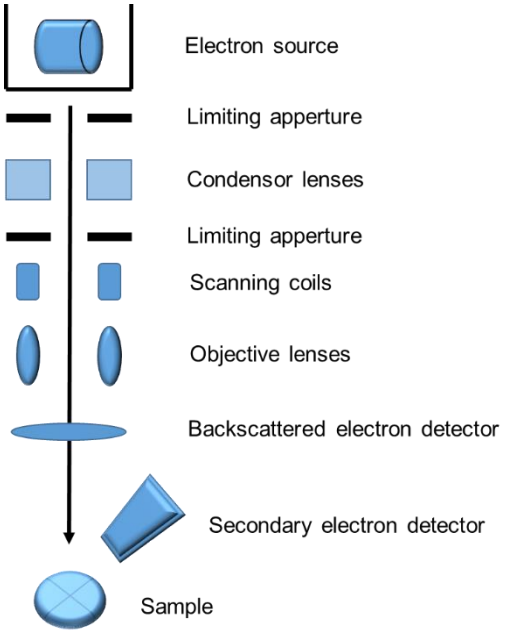

Figure 2.1– Schematic diagram of a Scanning electron microscopy (SEM) device. Adapted from [88].

Non-conductive materials have to be coated with a thin, electrically grounded layer of metal such as gold or by a non-metal as carbon. This layer diminishes the negative charge of the electron beams irradiating the sample's surface. The coating procedure has some disadvantages: at higher magnifications the image may be from the metal instead of the sample and if the layer's thickness is more than 200 Å, the electron beam may not reach the material in an EDS analysis. [49]

SEM (Zeiss Auriga at CENIMAT|I3N), was used to study the size and shape of nanocrystalline cellulose obtained at different acid hydrolysis times. An electron beam with 2Kv was applied to the samples with an aperture size of 30 μm. An aqueous suspension of NCC was placed in circular transmission electron microscopy (TEM) grids. The water of the sample was completely dried at room temperature and coated with carbon (thickness layer 20 nm). The lengths and diameter of individual nanoparticles, observed in the SEM images, were measured using ImageJ software (version 1.48, http://imagej.nih.gov/ij/)). The distribution of the particles length and width were achieved with 100 measurements.

3.4. Polarized Optical Microscopy (POM):

Polarized optical microscopy (POM) is widely used to characterize materials with optical properties like chiral nematic liquid crystals. A schematic of a polarize microscope is represented in figure 2.2. A halogen light bulb produces unpolarised beams, which are reflected by a mirror and pass through the lenses. The beams reach a polarizer that can rotate until 360°, followed by a condenser that uniforms the light that reaches the sample. After passing the objectives, a

second polarizer called analyser, absorbs almost all the light and only the beams that passed through an anisotropic environment are displayed, otherwise dark background is shown. A digital camera is used to record images of the samples and is placed above the objectives and the image is acquired by a semi-transmitting mirror. [89]

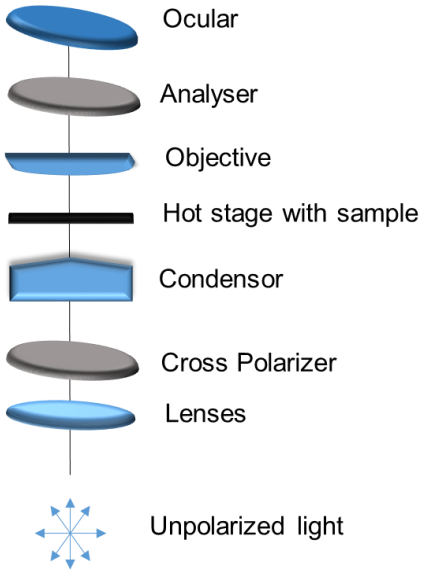

Figure 2.2 – Schematic of a polarized optical microscope. Adapted from [90].

Polarized optical microscopy was used to observe liquid crystalline textures in NCC/PVA and NCC/glycerol gels. To analyse the liquid crystalline phases a 90° difference between the analyser and the first polarizer had to be settled, this is, the image was acquire between cross polarizers. In the LC phase, the light is scattered according to the pitch of the sample and only the beams parallel to the analyser are observed. Optical microphotographs of the samples were taken using a transmission mode in an Olympus BX51 microscope coupled with an Olympus DP73 camera (CENIMAT|I3N) and Olympus BX50 at INEB. The pitch from the fingerprint texture observed in the acquired images was measured with the ImageJ software. The distribution of the pitch values was achieved with 100 measurements in each condition.

3.5. Transmission electron microscopy (TEM):

Transmission electron microscopy (TEM), provides information about the internal structure of the materials, inaccessible by other techniques such as POM or SEM. TEM is widely used to characterize materials or particles from the atomic to a micrometre level. A scheme of the transmission electron microscope is shown in figure 2.3. A high energy electron beam is produced by heating a cathode which can be a filament or a sharply pointed rod of a metal such as tungsten. The electrons collide with the anode, a disk with an axial hole configuration. The intensity and angular aperture of the electron beam is controlled by condenser lens. [91] A TEM image is

formed by transmission electrons, meaning, the electrons pass through the sample due to its thickness or transparency. The collision of these electrons with a fluorescent screen or a CCD generates the image. Black and white images are created. The black images occur when few electrons are transmitted. On the other hand, white images are created when a large number of electrons pass through the sample, thus are transmitted.

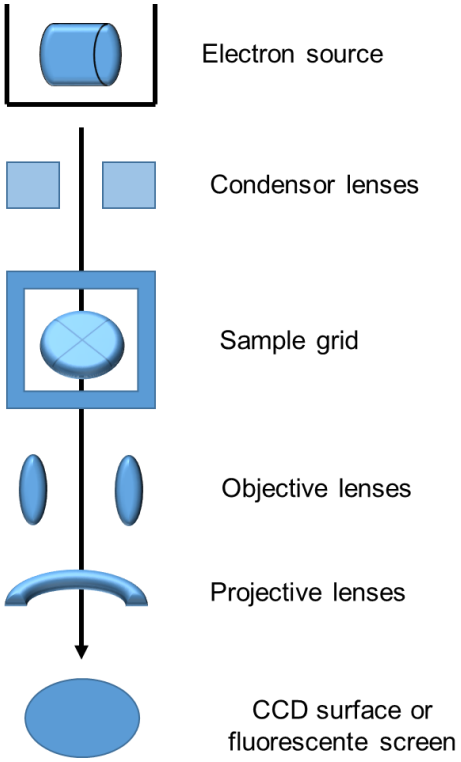

Figure 2.3 – Schematic diagram of a Transmission electron microscopy (TEM) device. Adapted from [88].

TEM enables the assessment of chemical compounds present in the sample and the crystallinity of the material. The sample preparation for TEM is a very complex procedure: the sample has to be completely dried due to the propagation of the electron beams and so vacuum was applied. Furthermore, the specimen has to be very thin so it has lower resistance to the electrons ("electron transparent") and has to be resilient to the high energy electron beams. [92]

Electron microscope Jeol JEM 1400, Zeiss model EM 10C and model EM 902A with a SC1000 OriusTM CCD camera gatan images were used to study the internal structure of the NCC/PVA gels. The sample was coated with EPON resin and an electron beam with 100 keV of energy was applied.

4. Integrity tests:

4.1. Non-mobility test:

After total removal of water from the NCC/glycerol gel, these were inverted and placed at rest during two weeks.

4.2. PBS stability test:

In order to understand the stability of the gels described in 1.3 was executed a simple test. The test consisted in placing 1ml of PBS, mixed with a yellow food dye, on top of a gel, placed in a vial. The set was closed and incubated at 37º C during six days. The test was performed in both NCC/glycerol and NCC/PVA gels. If the form and shape of the gels remain constant after this PBS stability test, a non-mobility test was conducted to the NCC/glycerol gels (see 4.1).

4.3. pH and culture medium stability test:

This test was carried out with the objective of increasing the pH of the NCC/glycerol gels to a suitable pH for cell culture and to ensure the stability of the gels after this procedure.

To increase the pH of the NCC/glycerol gels to a pH of 7, 1ml of PBS was deposited in the top of the gel and incubated at 37ºC for 4 hours and then the PBS was removed. The procedure was repeated four times, wherein the gel was left in the incubator overnight in the last procedure. The experimental work was performed in a 0.04% CO_2 atmosphere incubator.

To determine the behaviour of the NCC/glycerol gels in cell culture medium as well as the pH of the gel after this treatment, 1ml of cell culture medium was added to the gel and the set was incubated at 37ºC during 24 hours in an atmosphere of 5% CO_2. The same procedure was repeated in a 0.04% CO_2 atmosphere.

pH measurements were performed with a pH micro probe from Lazar Research laboratories, model PHR-146B, that can be observed in figure 2.4. Calibration of the equipment was executed previously to any measurements using the appropriate standard solutions.

To determine any changes in the chiral nematic structures of the NCC/glycerol gels after this treatments, the samples were observed by POM, in an Olympus BX50 microscope and the pitch measured by the ImageJ software. For statistical purposes 100 measurements were obtained.

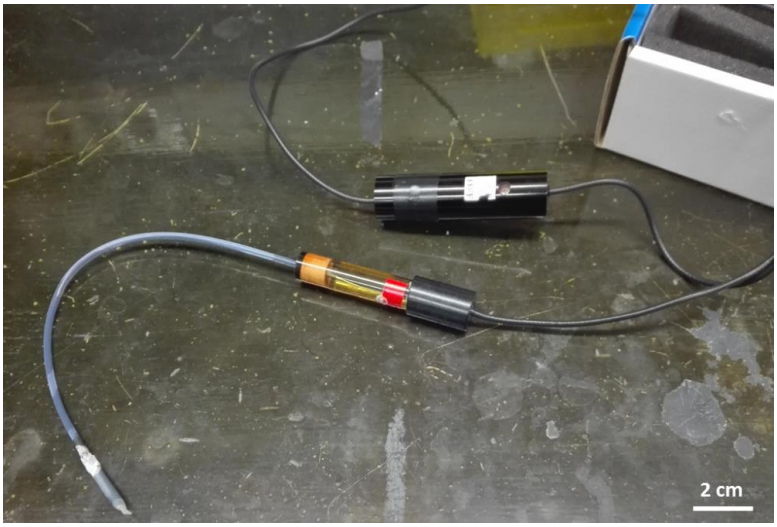

Figure 2.4 – pH probe used to measure the pH of the gels during the pH integrity test.

4.4. Swelling behaviour evaluation:

NCC/glycerol gels were submerged in PBS at 37ºC and weighted at precise time intervals. An attempt to remove the excess of water from the samples surface was done by placing the sample within filter papers.

5. Chemical analysis of the NCC/glycerol gels:

5.1. Electro kinetic Analysis (EKA):

An electro kinectic analyser measures the zeta potencial of a macroscope material. An electrolyte solution is pumped through a measurement cell containing the sample to measure. If the material is electrically charged, an electrochemical double layer is formed. This electrochemical double layer is divided in two: the immobile Stern layer, which is constituted with counterions (ions with opposite charge to that of the surface) and, closely to the Stern layer, the Gouy-Chapman layer that is a diffuse layer with both positive and negative charged ions. A plane of shear separates the two layers and the electrostatical potential in these planes is called the zeta potential. [93][94] An Anton Paar Electro Kinectic analyser was used to measure the 7% NCC/glycerol gels zeta potential, before and after 24 hours of incubation of the samples with cell culture medium. Six measurements were performed to ensure statistical viability of the results.

6. Rheology

The rheological properties of the NCC/glycerol gels: NCCs40'; NCCs70' and NCCs130' were studied with a rotational rheometer, (Kinexus Pro, Malvern Instruments, Malvern, UK). A brief explanation of the theory behind the methodology used is described in the supporting information (Annex I). For both viscometry and oscillatory measurements, the samples were allowed to rest after loading, for at least 30 min, before start applying any deformation.

6.1. Viscometry measurements:

Viscometry assays to the gels were performed using a cone (Ø 40 mm, 0.5°) and plate geometry, with a 0.015 mm gap and at 25°C, to assess the thixotropy of the gels through a hysteresis loop. This test was performed by means of an increasing ramp of shear rates (0.01 s^{-1} – 10000 s^{-1}), immediately followed by a decreasing ramp with the same shear rate values (Figure 2.5). The test was performed for a total of 10 minutes (5 minutes per shear rate ramp).

The dynamic shear viscosity of the samples could also be obtained from these assays. The area of the hysteresis loop is a measure of the thixotropic degree of the material, and depends on the experimental conditions such as test duration, maximum shear rate applied and shear history of the sample prior to the experiment. [95]

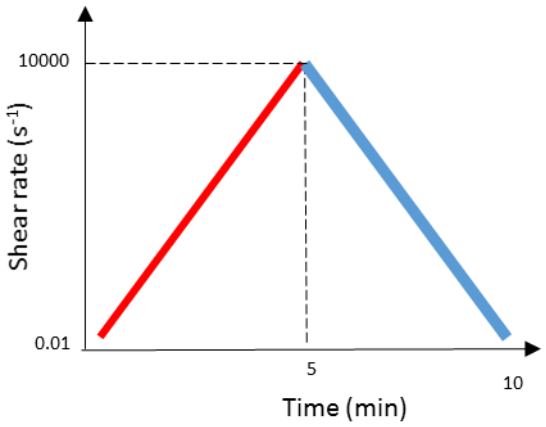

Figure 2.5 – Shear rate ramps applied to the sample for the hysteresis loop tests.

6.2. Oscillatory measurements:

The oscillatory tests were performed using a parallel plate geometry (Ø 20 mm) and a gap of 0.75 mm, at 25°C. Preliminary studies were done to determine both stress and frequency values within the linear viscoelastic region (LVR) of the gels. This region represents the stress and frequency windows at which the viscoelastic properties of the gels are independent of the stress or the frequency applied. After determining the LVRs of the gels, oscillatory frequency sweeps

were performed from 0.01 Hz to 50 Hz to determine the behaviour of the material with the increasing of the frequency applied as described in the literature.[96] In addition, oscillatory stress sweeps from 1 Pa to 4000 Pa, immediately followed by an oscillation test with fixed frequency and stress within the LVR of the gels for 5 minutes, were conducted as represented in figure 2.6 - A. This stress sweep test was adapted according to Shona Pek at al., that studied the effects of a thixiotropic matrix to posteriorly use in mesenchymal cells [97]. With these assays, it was assessed the ability of the gel to return to its initial viscoelastic properties after a transition to a liquid state. Both the yield stress and the complex shear stress of each gel needed for a solid-liquid transition of the material to take place were also determined.

A test sequence was designed to study the ability of the gels to recover the solid like properties after being stressed with a high shear stress value (out of the LVR and that allows a solid-liquid transition) as performed by Sharma et al.[98] The sequence (Figure 2.6 - B) was repeated 15 times for each gel and consisted on applying a shear stress (out of the LVR) for 1 min, followed by the application of a different shear stress (within the LVR) for 4 min.

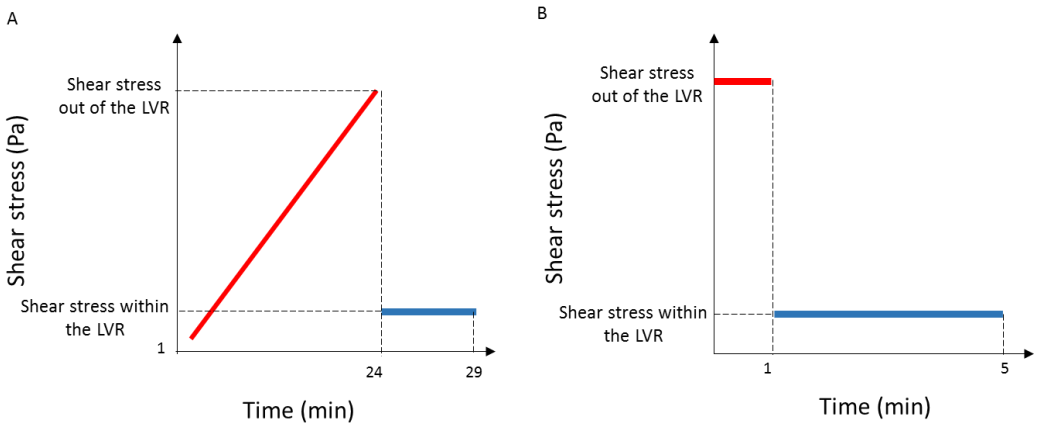

Figure 2.6 – Oscillatory assays performed to the gels. A - Oscillatory stress sweep, followed by an application of the LVR conditions. B - Oscillatory test in which a shear stress out of the LVR is applied for 1 minute followed by the application of a shear stress within the LVR for 4 minutes; this was repeated 15 times for each gel.

To study the differences of the viscoelastic properties of the gels after cell culture conditions (48 hours in cell culture medium), was used a fixed frequency and a fixed shear stress within the LVR of the gels, previously determined. The gel was placed in a gel caster (QGel® 3D disc casters (Lausanne, Switzerland) and incubated in the conditions described in section 4.3. After incubation, gel discs were cored out with a biopsy punch cylinder of 8 mm of diameter. For the oscillatory measurements, a parallel plate geometry (Ø 8 mm) was used with a 1.5 mm gap due to the use of the gel caster with the same diameter.

Each test was performed three times and both numeric and graphic results are represented as average ± standard deviation.

7. Cell culture

7.1. Specific cell-culture gel preparation methods:

All samples (NCC/glycerol gels: NCCs40', NCCs70' and NCCs130') were sterilized using two cycles of UV irradiation (15 minutes each) inside the laminar flow hood. After allowing the gels to reach the cell compatible pH range (pH equilibrium method described in section 4.3) these samples were used to perform cell adhesion and cytotoxicity tests.

7.2. Cell culture:

Cryopreserved Human Neonatal Dermal Fibroblasts (HNDF) were expanded. The HDNF were previously stored at -80°C in a cryovail. 8 mL of Dulbecco's modified essential culture medium with 10% FBS - fetal bovine serum and 2% of Pennicilin/Streptomicin were added to a T75 flask. The cryovail was immediately placed in a 37°C water bath for 1 minute without submerging the cap of the vial. The cryovail was rinsed with 70% ethanol and taken to a laminar flow hood where 1mL of pre-warmed culture medium was added to the cryovail. Slighted agitation was done to the cryovail content and the cells were transferred to the T75 flask. The cells were incubated for 8 hours at 37°C in a 5% CO_2 and the medium was replaced.

The medium was aspirated and the fibroblasts were washed 2 times with sterile PBS for the removal of fetal bovine serum traces. The PBS was removed and the cells were released from the flask bottom by adding a solution of 0.25% trypsin/2.21 mM EDTA. The cells were allowed to trypsinize for 5 minutes at 37°C. The trypsin was neutralized with 5 mL of DF-1 (Dermal fibroblast culture medium). To ensure the detachment of the cells from the bottom of the flask, microscopic visualization was performed and cells were counted. The cells were placed in a humidified incubator at 37ºC and 5% CO2. DF-1 was replaced every 3 days until the desired confluence was reached.

7.3. Cell Adhesion:

To perform the cell adhesion experiments, HNDF were seeded onto the surface of the gels and incubated during 24h at 37°C in 1mL DMEM (Dulbecco's Modified Eagle Medium) + 10% FBS. After the 24 hours of incubation, the culture medium was discarded and the remaining non-adherent cells were washed with PBS. As a control, gels with no cells were incubated and the metabolic activity was measured by a resazurin assay.

7.4. Citotoxicity assays:

The *in vitro* cytotoxicity tests were performed to determine the biocompatibility of the NCC/glycerol gels. Cytocompatibility of NCC gels was evaluated through both direct contact and indirect contact cell viability assays.

In the indirect contact assay, each well plate containing the gels was incubated during 24h at 37°C in 1mL DMEM + 10% FBS. After this incubation, the media was collected and used to cultivate HNDF previously seeded on a 24 well plate to a final concentration of 10000 cells per well. As a control, the same number of cells were cultured using fresh medium. After this period the metabolic activity was assessed by resazurin assay.

In the direct contact test, each gel was incubated on top of pre-seeded HDNF in a 24 well plate (10000 cells/ well) during 24h and 48h at 37°C in 500 μL DMEM + 10% FBS. As a control, the same number of cells without addition of the gels was used. After this period the metabolic activity was assessed by resazurin assay.

7.5. Resazurin metabolic test:

A resazurin assay offers a simple method to measure the metabolic activity of living cells. This metabolic activity causes a reduction in the resazurin to resorufin. Resorufin emits fluorescence at 590 nm which is measured by a spectrophotometer. These tests are not destructive due to the non-toxicity of resazurin and its derivatives and their stability in culture medium. [99]

Resazurin was diluted (20% v/v) in the respective medium (DMEM+10% FBS) and samples were incubated for 3 h at 37°C. A fluorometer (Synergy Mx o, Biotek) was used to excite the samples at 530 nm and read the fluorescence at 590 nm. DMEM+10% FBS with resazurin (20% v/v) was used as blank samples.

To measure the metabolic activities in cell adhesion and in both direct and indirect methods the culture medium was retrieved and, in the direct contact test, the gel was also discarded. The results obtained are presented in terms of relative metabolic activity with metabolic activity of control considered as 100%. Averages and standard deviations are reported. All data were analysed using the Mann-Whitney U test with Graph Pad Prism 6 software.

Chapter III - Results and Discussion

Having in mind the objectives of this dissertation, several attempts were performed to produce nanocrystalline cellulose (NCC) based gels with liquid crystal properties. Glycerol and polyvinyl alcohol (PVA) were the materials selected as a polymer matrix to produce these gels and NCC with different sizes were produced and characterized. In order to produce these gels, different NCC contents were also used and its influence on the liquid crystalline phase, estimated by the pitch of the fingerprint textures, evaluated by microscopic techniques. An attempt to obtain collagen gels was also performed.

The gel stability, when in contact with culture medium, was evaluated with a set of integrity tests specially developed. The gels' pH was increased to allow its use in fibroblast cell culture.

For a better characterization of the NCC/glycerol gels, preliminary rheological studies were performed as well as the study of modifications in chemical and rheological properties of the gels after the contact with culture medium.

To assess the possibility of using NCC/glycerol gels as a biomaterial unravelling its LC characteristics, exploratory cell culture tests were conducted.

1. NCC synthesis and characterization

1.1. Synthesis:

Nanocrystalline cellulose was successfully synthesized from the acid hydrolysis reaction of the microcrystalline cellulose with the sulfuric acid, as shown in the scheme represented in figure 3.1.

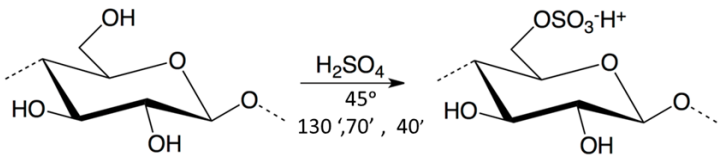

Figure 3.1 – Schematic representation of the acid hydrolysis reaction of micro-cellulose to afford nanocrystalline cellulose with sulfate half-ester groups in an acid form.

It is considered that cellulose chains are assembled in alternating rigid (crystalline) and flexible (amorphous) regions. [85] In this reaction the more accessible amorphous regions undergo chemical attack with the sulfuric acid and as a consequence particles with smaller sizes and higher crystallinity can be extracted from the reaction medium. This nanoparticles have sulfate half-ester groups that were added to the active -OH sites of cellulose in the acid form.

1.2. Characterization:

In figure 3.2, it can be seen the ATR-FTIR spectrum of a NCC film obtained by solvent casting of an aqueous NCC suspension with 2.5% (w/w) of solid content. In this figure it is noticeable the characteristic FTIR peaks of cellulose, this is, the stretching vibrations of the bond type O–H, CH and C–O at approximately 3400 cm^{-1}, 2900 cm^{-1} and 1060 cm^{-1}, respectively. Also a peak associated with the bending vibration of the O-H bond at approximately 1640 cm^{-1} wavenumber is present, in good agreement with spectra of the nanocrystalline cellulose obtained from similar source. [84] The existence of peaks in the range of 700-650 cm^{-1} can be assigned to S–O bond bending due to the presence of sulfate groups in the NCC surface.

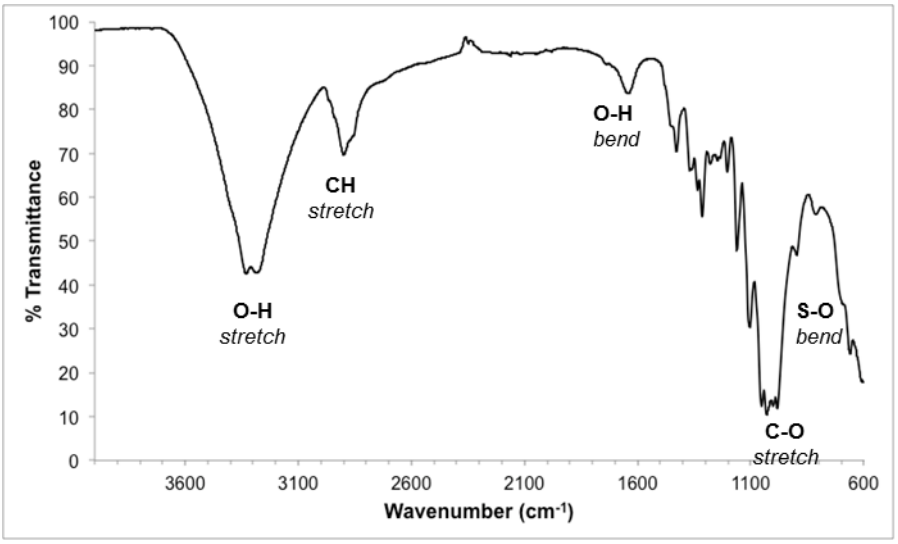

Figure 3.2 – ATR-FTIR spectrum of a thin film of nanocrystalline cellulose obtained by the reaction of acid hydrolysis of microcrystalline cellulose during 130 min.

X-ray diffractometry was used to analyze the crystallinity index and crystallite size of both NCC and its source MCC. The diffractograms are shown in figure 3.3. From this figure it can be seen that both materials show the same diffraction features as the ones observed for semicrystalline cellulose type I. [84] The main characteristic crystallography planes or cellulose type I are $1\bar{1}0$, 100 and 200 and in our samples 2θ is at 14.7º, 16,8º and 22.7º, respectively.

From the X-Ray diffractogram the crystallinity index I_c was determined considering the following empirical method develop by Segal et al. [100]:

$$I_c = \frac{I_{002} - I_{min}}{I_{002}} \times 100$$

where, I_{002} represents the maximum intensity of the crystalline region, at a 2θ angle between 21° and 23º, and I_{min} represents the intensity of the amorphous region defined as the minimum value at a 2θ angle between 18º and 20º.

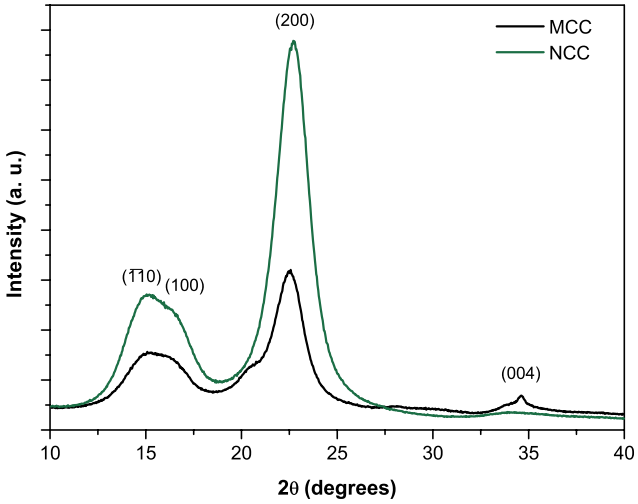

Figure 3.3 – XRD diffractograms of unmodified microcrystalline cellulose (MCC) and NCC obtained at 130 min of acid hydrolysis reaction time. The characteristic peaks of cellulose type I are highlighted in the diffractogram.

The crystallite size of the cellulosic materials could be determined using the Scherrer equation [101]:

$$D_{hkl} = \frac{0.9\,\lambda}{\beta \cos\theta}$$

where, D_{hkl} is the crystallite size in the directional normal to the hkl lattice planes, λ is the x-ray wavelength, β is the full width at half-maximum (FWHM) of the diffraction peak and θ is the corresponding Bragg angle.

Table 3.1 summarizes the values of I_c and D_{hkl} and it can be seen that the acid hydrolysis reaction leads to an increase in the crystallinity index of NCC and a slight decrease in the crystalline size. From the values presented in the table 3.1 one could expect to obtained intermediate values of crystallinity index I_c and crystalline size for the NCCs obtained with the other hydrolysis reactions times. Nevertheless, this characterization was only performed with the intent to show a change in these characteristics.

Table 3.1 – Crystallinity index and crystallite size calculated from the x-ray diffractograms for MCC and NCC obtained with 130 minutes of acid hydrolysis.

Cellulose type	2θ (I_{002})	I_c (%)	D_{hkl} (nm)
MCC	22.60	76.73	5.39
NCC 130'	22.70	87.80	4.79

In figure 3.4, which presents SEM images of nanocrystalline cellulose films obtained from NCC suspensions, it is observed that NCC exhibited a nano rodlike shape in every acid hydrolysis performed (40, 70 and 130 minutes) in good agreement with the observed by other authors. [84]

Measurements of width and length, performed with ImageJ software, are presented in table 3.2. It can be seen that the overall aspect ratio of the NCC is not greatly affected with the increase of the hydrolysis times and the same can be said to the nanoparticles diameter. Nevertheless, the increase of hydrolysis time from 40 to 130 minutes leads, as expected to a 1.75 times reduction of the NCC length. In annex I (figure A2) a plot of the effect of acid hydrolysis time on the length of NCC is plotted with date from Dong et al.[5] The experimental results obtained in this work with the hydrolysis time of 40 and 210 minutes are in good agreement as the ones reported in the literature, however the average length obtained for the hydrolysis reaction time of 70 minutes is slightly higher than the expected. In order to try to understand this difference, another set of SEM images and measures should be obtained and a different hydrolysis reactions times should be used. Nevertheless and having in mind the goal of this work, the results obtained were enough to observe a reduction in the NCC length with the increase of the acid hydrolysis reaction time.[5]

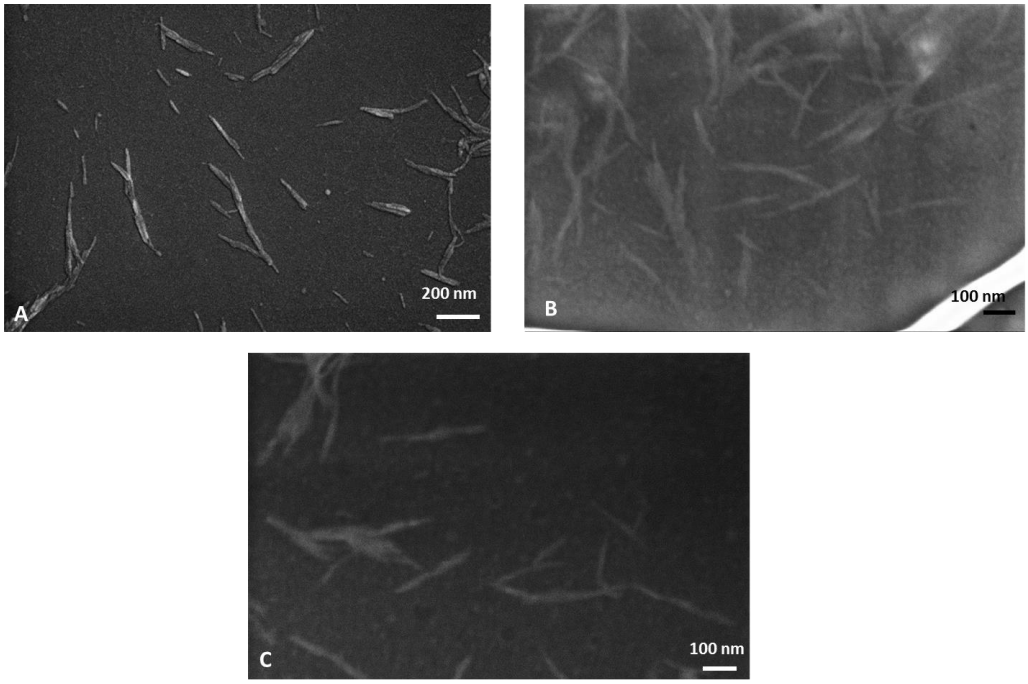

Figure 3.4 – SEM images of nanocrystalline cellulose obtained from reactions with different acid hydrolysis time, taken with a 75K magnification. A, B, C show NCC obtained at 130 min, 70 min and 40min. acid hydrolysis time, respectively.

Table 3.2 – Measurements of width and length of NCC obtained with different hydrolysis time.

Acid hydrolysis time (minutes)	Width (nm)	Length (nm)	Aspect ratio (L/D)
40	24±8	244±88	10
70	24±8	231±85	10
130	18±8	163±75	9

The sulfate groups present in the cellulosic chain are considered to be responsible for the lowering of the nanocrystalline particles aggregation, resulting in the development of stable dispersion of NCC in water. This suspension can, when the amount of NCC is above the critical value, present birefringence, as can be seen in figure 3.5, which coexists with the isotropic phase. This birefringence is characteristic of the liquid crystalline phases of NCC. [84]

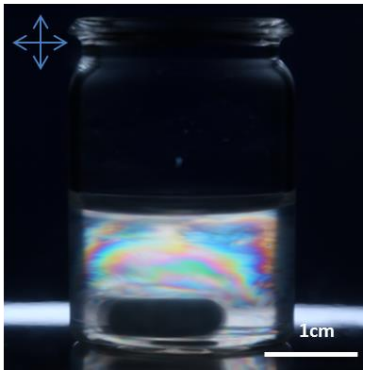

Figure 3.5 – Photograph of a 2.12% (w/w) NCC aqueous suspension showing birefringence, characteristic of the presence of a LC phase, resultant of the reflection of light of the suspension observed between cross polarizers.

2. Structural characterization of NCC gels

2.1. NCC/glycerol and NCC/PVA gel formation:

The gelation of NCC with glycerol, following the method described by Dorris et al. was successfully achieved. [87] NCC/glycerol gels with 3, 5, 7, 10 and 18 % (w/w) of NCC were prepared, and in figure 3.6, it can be seen a photograph of a gel with 7% NCC content (w/w).

Figure 3.6 – NCC/glycerol gel with 7%NCC content (w/w) in the gel.

NCC/PVA gelation was also successfully performed by consecutives freeze-thawing cycles following the method described by Abitbol et al. [58] and the visual aspect of the gels is shown in figure 3.7. From this figure it can be seen that the gels with higher amount of NCC are less stable than the ones with lower NCC content.

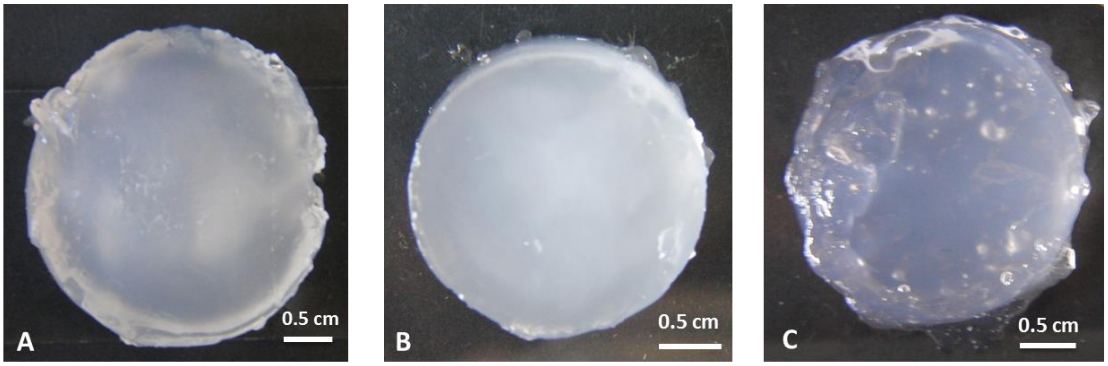

Figure 3.7 – Photographs of the NCC/PVA gels with different NCC/PVA ratio. NCC content % (w/w): A – 0.65%, B – 4.85% and C – 10%. All percentages of NCC presented are with regarding to the dry weight of PVA.

2.2. Polarized Optical Microscopy (POM):

NCC/glycerol, as well as, NCC/PVA gels do not present birefringence when observed with cross-polarizers without magnification. Nevertheless, birefringence was detected in both gels when the samples were observed with an optical microscope with cross-polarizers (figure 3.8).

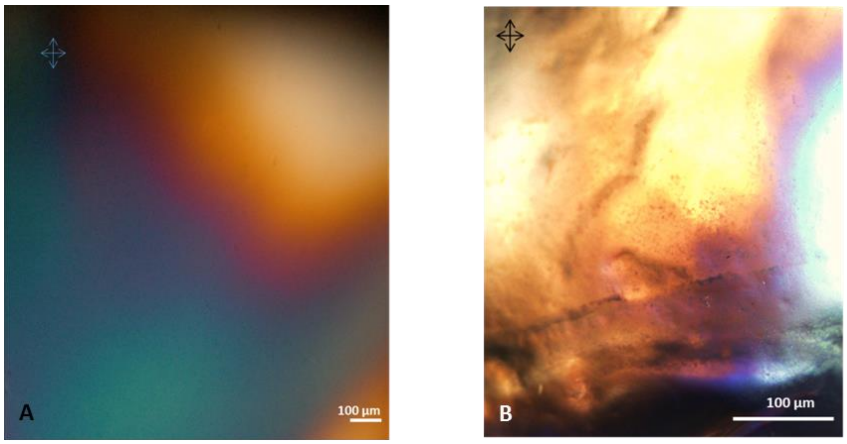

Figure 3.8 – Photographs obtained with POM taken between cross polarizers and a 20x magnification. A – NCC/glycerol gel with 5% (w/w) NCC; B – NCC/PVA gel with 4.85% NCC dry weight of PVA.

In NCC/glycerol gels with NCC concentration higher than 7%, a fingerprint texture appeared, as can be observed in figure 3.9. These fingerprint textures are typical of a liquid crystalline phase of NCC as presented by Revol et al. [84], among others, characteristic of a chiral nematic liquid crystalline phase. This texture is formed by an arrangement of intercalated anisotropic band (bright) and an isotropic band (black). The presence of a chiral nematic phase

in the gels and mainly the appearance of fingerprint textures with a micrometric size pitch will allows us to control, by an inexpensive and easy method (POM), possible changes in the LC phase after doing cell culture tests. More important this evidence will help us understanding the influence of the gel's organizational order on the cellular growth, mainly if a specific cellular differentiation is achieved.

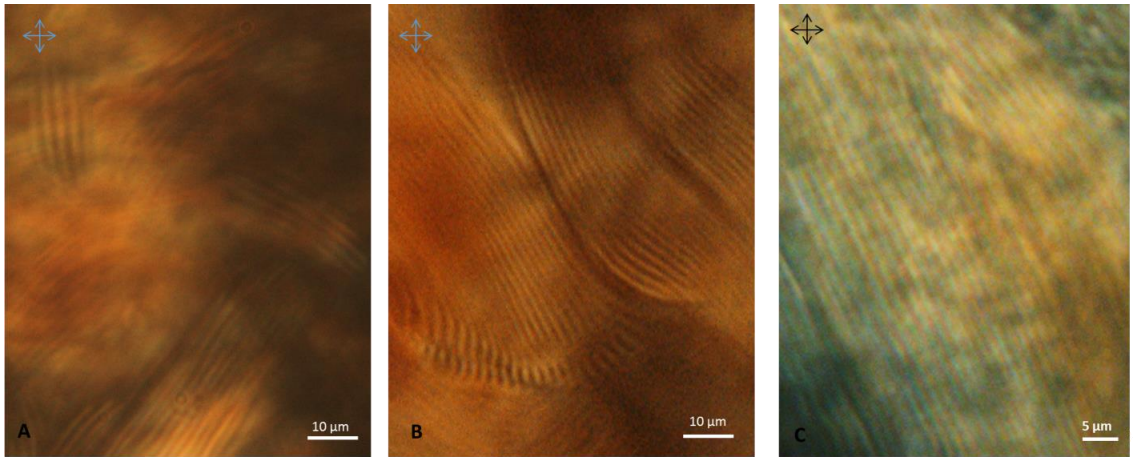

Figure 3.9 – Pictures of NCC/glycerol gels (130 minutes acid hydrolysis time), observed through POM with cross polarizers with a 20x magnification. A – NCC/glycerol gel with 7% (w/w) NCC; B – NCC/glycerol gel with 10% (w/w) NCC; C – NCC/glycerol gel with 18% (w/w) NCC.

To study the influence of the NCC length size and content in the gels, the measurement of the band-spacing (half the cholesteric pitch) of the fingerprint texture was performed with ImageJ software. The measurements are summarized in table 3.3. These results indicate a slight decrease of the pitch with the increase of the NCC content in the gel. In contrast, the pitch decreases 3 times when NCC particles with almost half of the size are used. In the figure 3.10, it can be see POM pictures of the gels with shorter hydrolysis time (NCCs40' and NCCs70') and its noticeable a fingerprint textures with higher pitch values (the bands are thicker) than the ones observed for gels of NCCs130'. These values are within the same range (1-15µm) to those found in literature concerning a chiral nematic liquid crystalline cellulosic phase. [84] [102] Furthermore, the relationship between the NCC length and the acid hydrolysis reaction time observed by Beck-Candanedo et al. was obtained in our gels, where higher NCC length, shorter acid hydrolysis reaction time, leads to higher pitch values.[103]

Table 3.3 – Pitch measurements on NCCs/glycerol gels.

NCCs % (w/w)	Acid hydrolysis time (min)	Pitch (µm)
7%	NCCs40'	14±1
	NCCs70'	11.0±0.9
	NCCs130'	4.4±0.4
10%	130	4.0±0.3
18%	130	2.8±0.3

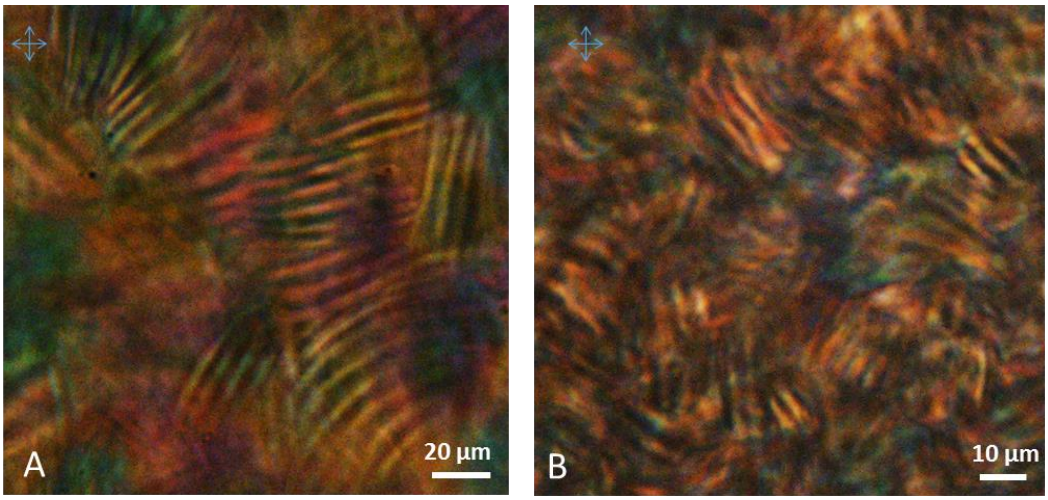

Figure 3.10 – Pictures of NCC/glycerol gels with 7% (w/w) NCC content, observed through POM with cross polarizers and a 20x magnification. A – NCCs40' gel; B – NCCs70' gel

2.3. Transmission electron microscopy:

Since no fingerprint texture was observed in the NCC/PVA gels by POM another microscopy - TEM - was used. Figure 3.11 shows TEM images of the surface of a NCC/PVA gel sample with 4.85% (w/w) of NCC. It is important to note that gels with other NCC content were damaged in the sample preparation procedure, and could not be observed by TEM. Also during this examination some samples were deteriorated by electron beam irradiation. From the TEM images, it is not possible to see any specific type of organization.

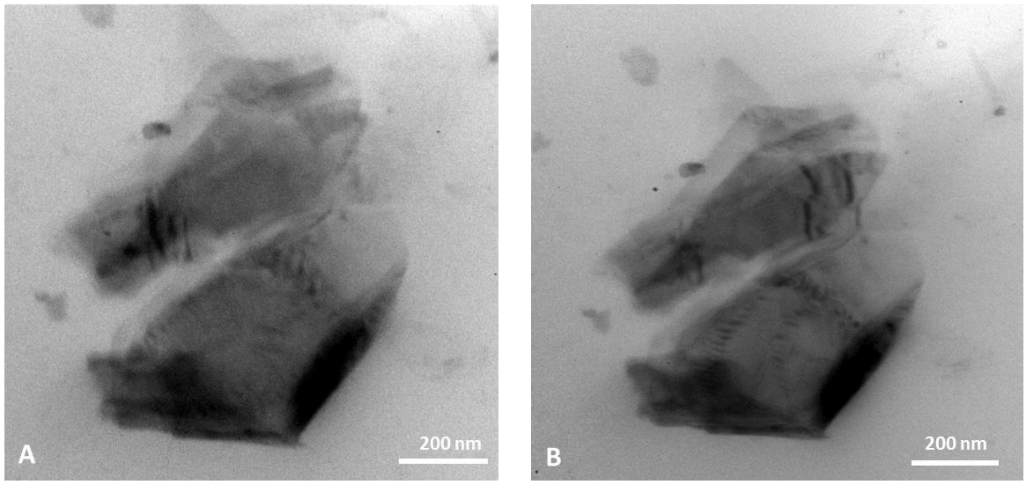

Figure 3.11 – Pictures of NCC/PVA gels with 4.85% (w/w) NCC of the dry weight of the polymer.

3. Integrity tests:

To confirm the integrity of the NCC/glycerol gels as well as the NCC/PVA gels, were performed several tests, described below: PBS stability test, non-mobility test and pH stability test.

3.1. PBS stability test:

In figure 3.12 – A, it can be seen a gel of NCC/glycerol and in figures 3.12 B and C part of NCC/PVA gels that were in contact with PBS, with yellow dye, for several days. These photographs confirm that both NCC/glycerol and NCC/PVA gels do not disintegrate when in contact with PBS. Both gels present the yellow dye color within its bulk, which confirms that they are capable of swelling and absorb PBS into their network.

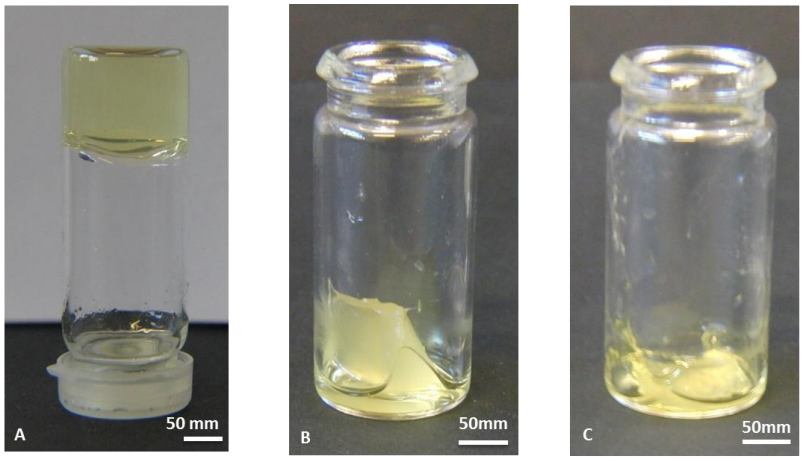

Figure 3.12 – Photographs of the NCC gels after the PBS stability test. The NCC/glycerol gel did not suffer any structural deformation. A – NCC/glycerol gel with 5% NCCs concentration; B and C are NCC/PVA gels with 0.65% and C with 10% of NCCs concentration regarding the PVA dry weight.

After 30 days of storage at 4°C the NCC/PVA gel showed signals of microorganism's activity. Consequently, and adding the absence of liquid crystalline characteristic textures, no more characterization or attempt to use in cell culture was executed in these gels.

3.2. Non- mobility test:

In the non-mobility test the vials of the gels were kept inverted for at least 2 weeks. In figure 3.13, it is possible to verify that the NCC/glycerol gels maintained its consistence and did not alter its position during this experience. In the images a black line marks the initial position of the gel and it was confirmed the absence of movement of the gel.

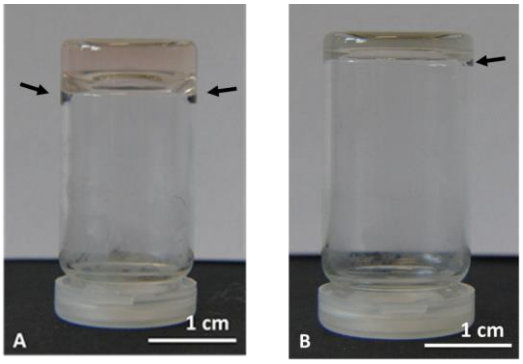

Figure 3.13 – Photographs of the NCC/glycerol gels after two weeks of inversion. The gels did not alter their position during the experience. In some photographs it is possible to observe a black mark of the initial position of the gel and confirm the absence of movement of the gel. A – NCC/glycerol gel with 5% NCCs concentration; B - NCC/glycerol gel with 10% NCCs concentration. The arrows mark the surface of the gel in the vial.

3.3. pH stability test:

This test was performed with the aim of understanding if NCC/glycerol gels (NCCs40', NCCs70' and NCCS130') are suitable for cell culture. Due to its low initial pH (~ 4-5) it was necessary to increase the pH of the gels since the ideal pH for the fibroblast cell culture is 7.4-7.7. [104]

The results for the pH equilibrium of the NCC/glycerol gel are shown in table 3.4 and as one can see, the increase of the pH of the gel was successful achieved, raising to a value of 8, making both protocols suitable to be used prior to cell culture procedures.

Table 3.4 – pH measurements of the NCCS/glycerol gels

Experimental Conditions	pH measured
PBS (0.04% CO_2)	8.25
Culture medium (5% CO_2)	8.77
Culture medium (0.04%CO_2)	8.36

It was observed a change of the gel color after incubation with the culture medium. This happened due to the presence of phenol red in the culture medium. If the pH is lower than 7.6 the phenol red turns yellow as visible in figure 3.14. On the other hand when the pH is above 7.6 the phenol red maintains its color. [104] This observation is in accordance with the initial acidity of the gel.

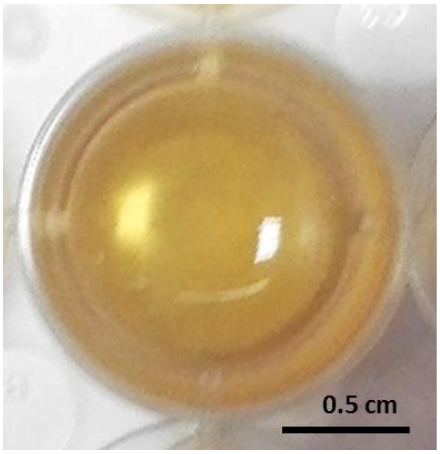

Figure 3.14 – Photograph of the NCC/glycerol gel after the pH stability test with cell culture medium. The gel changes the color of the medium due to its acidity.

In order to try to understand if the variation of pH would affect the LC properties, the fingerprint texture of the gels was observed by POM. As shown in figure 3.15, in both PBS (3.15 - A) and culture medium (3.15 B-D) pH stabilization, the fingerprints are still present in the NCC/glycerol gel. The fingerprint textures of the gel when pH equilibrated with PBS are faded in comparison with the fingerprint textures from the pH equilibration with culture medium.

Measurements of the pitch from the fingerprint texture observed after pH equilibrium with cell culture medium in the photographs presented in figure 3.15 are summarized in table 3.5. It can be seen that an increase in the pitch values is observed in every conditions of the gel when compared with the gels before the pH raise (see table 3.3). Having in mind the illustration presented in figure 1.2, for the organization of the chiral nematic LC phase, and the evolution of the pitch as function of the NCC content one can assume that the increase of the helical pitch, when in contact with cell culture medium, is derived from the presence of water and salts molecules (present in the medium) between the cholesteric layers. These molecules will affect the distance between the layers leading to an increase in its spacing and as a consequence, an increase in the pitch is observed. Furthermore from the results presented in table 3.5 it can be seen that the gel derived from NCC obtained at a higher hydrolysis time have an increase in the pitch value of 3.5 times, however for gels from NCC with lower reaction time the increment observed in the pitch value is only of 1.3 and 1.4 times. The unexpected behavior of the gel obtained with NCC with higher hydrolysis time should be further explored in order to be able to propose a valid explanation and also, more acid hydrolysis reaction times should be use in order to established a specific tendency of the influence of the culture medium in the pitch of the gels.

Table 3.5 – Pitch measurements of the NCC/glycerol gels before and after pH equilibrium with cell culture medium.

Gels	Pitch (µm) gels with pH=4	Pitch (µm) gels with pH ~8
NCCs40'	14±1	18±2
NCCs70'	11.0±0.9	15±2
NCCs130'	4.4±0.4	14±2

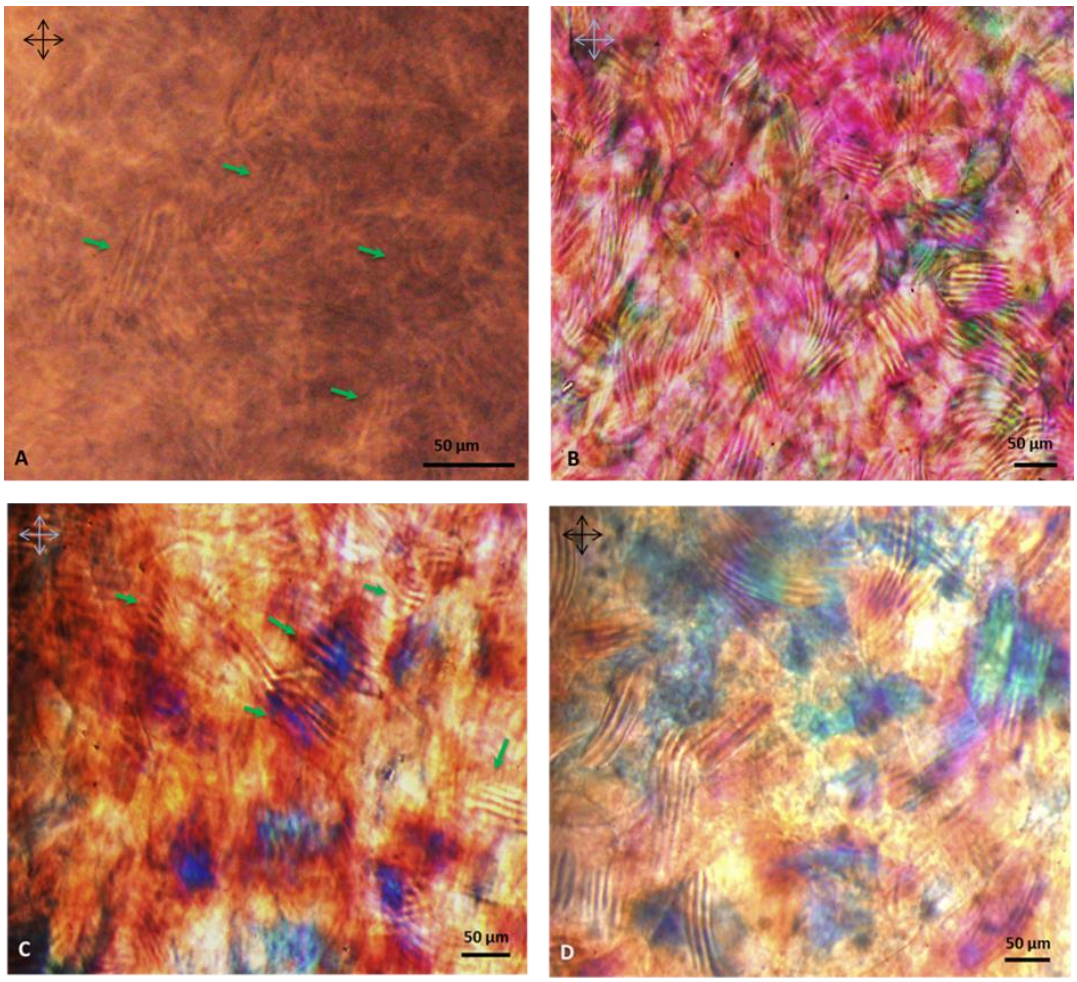

Figure 3.15 – Photographs taken through polarized optical microscopy with cross polarizers and 20X magnification of the NCC/glycerol gels after the pH stability test. A – "Fingerprint" textures of the NCCs130' gel after the pH equilibrium with PBS. B, C and D shows fingerprint textures from: A – NCCs130'; B- NCCs70'; C – NCCs40' with pH equilibrium with culture medium.

3.4. Swelling behaviour:

Several attempts were done to determine the swelling behavior of the NCC/glycerol gels, however the gels disintegrate during the test. With this outcome it was not possible to perform a swelling test with viable data.

3.5. Electro kinetic analysis (EKA):

Zeta potential is a highly used parameter that elucidates on the stability of the NCC dispersion in aqueous media and it is often used to understand the effect of acid hydrolysis reaction time in these suspensions. [105]

The results of the electro kinetic analysis of the NCC/glycerol gels are displayed in the table 3.6. In this study we have tried to infer on the influence of the acid hydrolysis reaction time, as well as the gel treatment with cell culture medium in the zeta potential values obtained for the gels.

Table 3.6 – Electro kinetic analysis results.

Gels	Incubation with culture medium	Zeta potential (mV)
NCCs40'	No	-8.4 ± 0.3
	Yes	-4.0 ± 0.4
NCCs70'	No	-11.2 ± 0.4
	Yes	-6.7 ± 0.7
NCCs130'	No	-4.0 ± 0.1
	Yes	-6.0 ± 0.2

The negative zeta potential of the gels possibly have origin in the negative charges of the nanocrystalline cellulose. NCC obtained by sulfuric acid hydrolysis have a negative zeta potential that differs with the purity of the sulfuric acid used as well as the acid hydrolysis times. Other studies shown that the zeta potential for NCC aqueous suspensions varies between -95.3 mV (120 min acid hydrolysis) to -8.77 mV (20 min acid hydrolysis).[105] Indeed, one observed an increase of the zeta potential in our results when the reaction time increases from 40 to 70 minutes. However the same trend is not observed for 130 min of reaction time. The zeta potential values obtained show that the NCC/glycerol gels are stable (if the zeta potential is above +30 mV or below -30mV the gel is unstable) [106].

A decrease in the zeta potential is seen in the NCCs40' and NCCs70' gels after the incubation with culture medium. This phenomenon can derive from the pH equilibrium described in the chapter II, section 4.3.

3.6. ATR-FTIR:

The effect of the increase of the pH, with cell culture medium, in the gels of NCC/glycerol was also explored by means of ATR-FTIR. In figure 3.16 are shown the FTIR spectra of NCC/glycerol gels, obtained with different NCC reaction times before and after the treatment with cell culture medium. From these spectra one can see that the characteristic bands of the sulfate group vibration (S=O at ~1100cm^{-1}) and bending (S-O at ~800 cm^{-1}) are not so strong in the

samples where the pH was raised, than in the samples that were not expose to the cell culture medium. This effect is observed for all the acid hydrolysis times studied and might be due to the substitution of the acid form of the sulfate group to a sodium form. All FTIR spectra also show the vibrational bands of the characteristic groups of cellulose and glycerol.

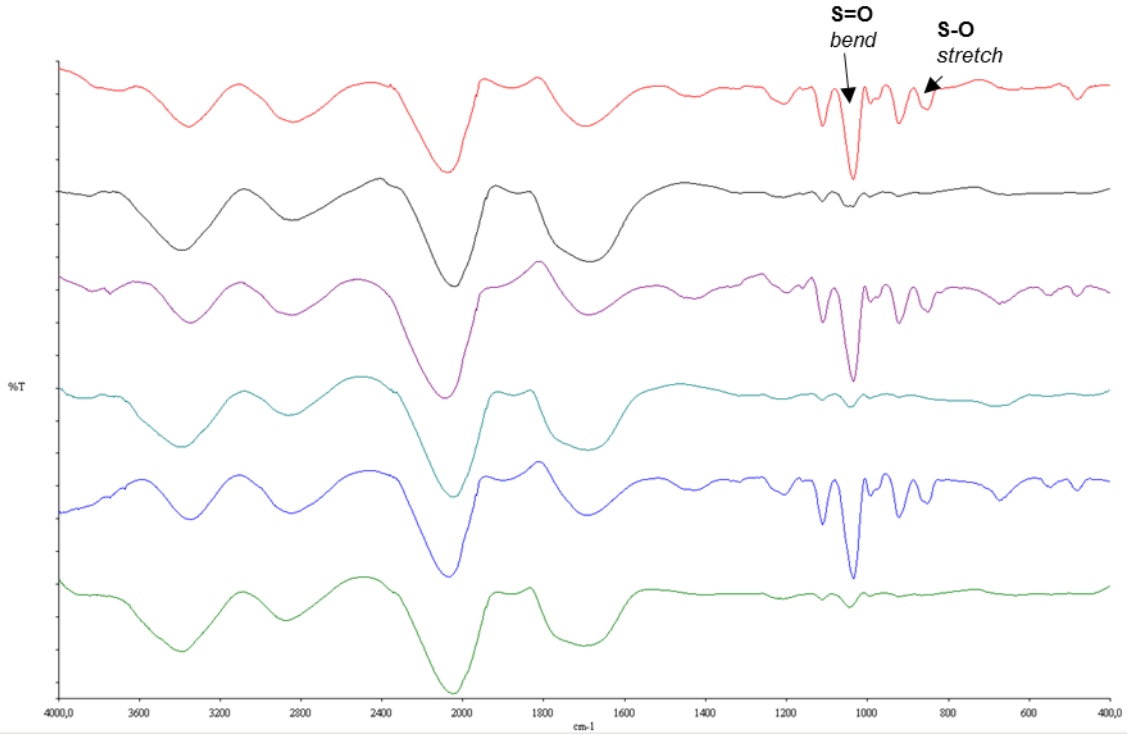

Figure 3.16 – ATR-FTIR spectra of NCC/glycerol gels. Red – NCCs40'; Black – NCCs40' with culture medium incubation; Purple - NCCs70'; Light blue – NCCs70' with culture medium incubation; Dark blue – NCCs130' and Green – NCCs130' with culture medium incubation.

4. Rheology:

A biomaterial has to be well characterized for future applications. Thus, understanding the thixotropic behaviour of the gels, along with its viscoelastic properties is essential. Additionally, the correlation of different nanocrystalline cellulose (NCC) sizes and consequently chiral nematic pitches with the rheological properties of each gel, can also aid in the study of liquid crystalline properties of the gels.

According to the literature [87], NCC/glycerol gels are thixotropic. IUPAC states that thixotropy is "the continuous decrease of viscosity with time when flow is applied to a sample that has been previously at rest and the subsequent recovery of viscosity in time when the flow is discontinued". [107] Thixotropic gels have the ability to become liquid-like materials when a high shear is applied, and to return to its original solid-like state after the stress is decreased or ceased. [108] Characteristically, these materials can, after the application of a shear outside the LVR (see

methods page 24) of the material, totally or partially recover the viscoelastic properties that they possessed before the shear was applied.

4.1. Frequency sweeps:

The data collected from the oscillatory tests (frequency sweeps and stress sweeps, Figs 3.17 and 3.20) performed to the gels revealed that a shear stress of 10 Pa and a frequency of 2 Hz are within the LVR of all NCC/glycerol gels. All subsequent oscillatory tests that applied LVR conditions used the values stated above of frequency and shear stress.

The results from oscillatory frequency sweeps tests, indicate that the viscoelastic properties of the gels remains stable (no phase transitions occurred), as a function of the frequency. This conclusion relies on the phase angle, which correlates the *G''* (loss modulus) and *G'* (storage modulus) values and also gives an insight regarding the more solid-like or liquid like-behaviour of the gels (see Annex I). The values of the phase angle are fairly constant throughout the frequency sweep tests.

In all samples the *G'* is higher than the *G"*, indicating a dominant solid-like behaviour, which is characteristic of most of gel like materials. In addition, the phase angle is lower than 45°, indicating the predominance of the more solid-like state of the material, independently of the frequency applied to the samples (see Annex I). The slight plateau of the *G'* that is visible in the first points of the frequency sweep graphics, also corroborates that the material tested is indeed a gel like material.

The different samples of NCC/glycerol gels also showed similar values of phase angle (Table 3.7). This is an indicator of an absence of remarkable differences in the ratio between the *G''* and *G'*. The NCCs40' gels present lower storage modulus values than the NCCs70' and NCCs130' gels, this is, the NCCs40' gels present a lower stiffness. The viscoelastic properties of the NCCs70' and NCCs130' gels are similar. The decrease in the NCC length seems to lead to an increase in the G' and G'' values, however from the results obtained in this study no linear relation is obtained. From table 3.2 we can highlight that the average value of the NCC length when 70 minutes of hydrolysis time is used instead of 40 minutes are very similar however the viscoelastic properties are not. This difference might be related with the fact that longer hydrolysis time leads to higher sulphate contents, as shown by Dong et al., [5] and that this groups will influence the ionic interactions between the polymeric chains and consequently the formation of the gel and its viscoelastic properties.

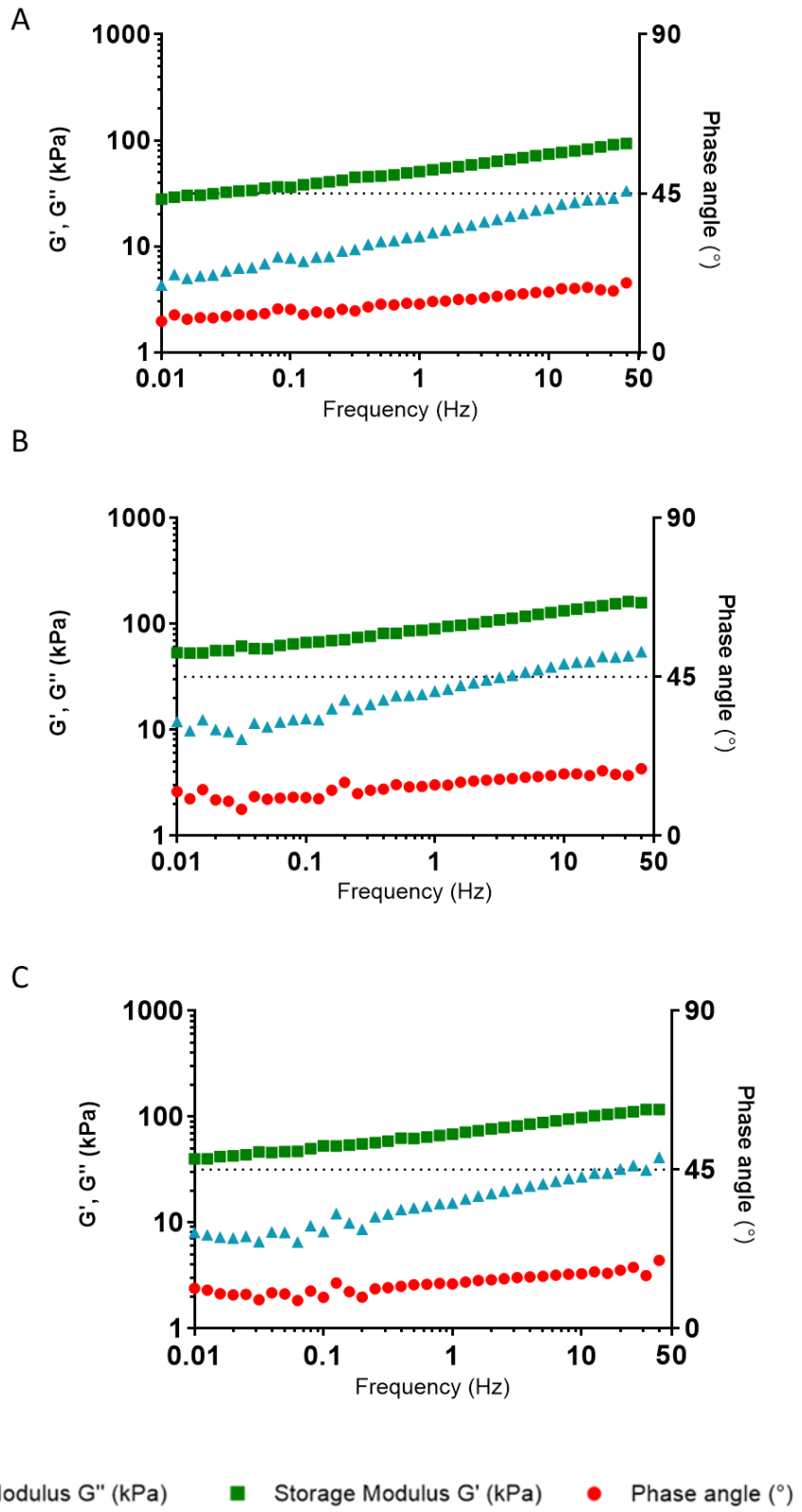

Figure 3.17 – Frequency sweeps of the NCC/glycerol gels with 7% NCC (w/w) (A - NCCs40', B - NCCs70' and C - NCCs130') with a fixed shear stress of 10 Pa.

Table 3.7 – Storage and Loss modulus and phase angle values of the of the NCC/glycerol gels with 7% NCC (w/w) (NCCs40', NCCs70' and NCCs130') from the frequency sweep measurements, at 2 Hz and using a 10Pa shear stress.

Gels	*G'* (kPa)	*G''* (kPa)	Phase angle (°)
NCCs40'	66 ± 10	19 ± 3	15.6 ± 0.9
NCCs70'	99 ± 16	28 ± 4	15.7 ± 0.2
NCCs130'	90 ± 16	24 ± 6	15.4 ± 1.4

4.2. Viscometry assays

For the hysteresis loop test, the maximum shear rate demanded to the rheometer (10000 s^{-1}), could not be achieved for all samples (Fig 3.18). This may arise from the high viscosity of the gels, which induces a high normal force on the test accessories when the samples are loaded and further during the assays. Due to shortness of time, only the hysteresis loop test with 600 seconds of execution was performed, although, according to literature, to avoid the effect of the inertia, the test time should have been calculated as: 1s per each $1s^{-1}$ of shear rate in the ramp. [108] Therefore the viscosity measurements should only be considered qualitatively.

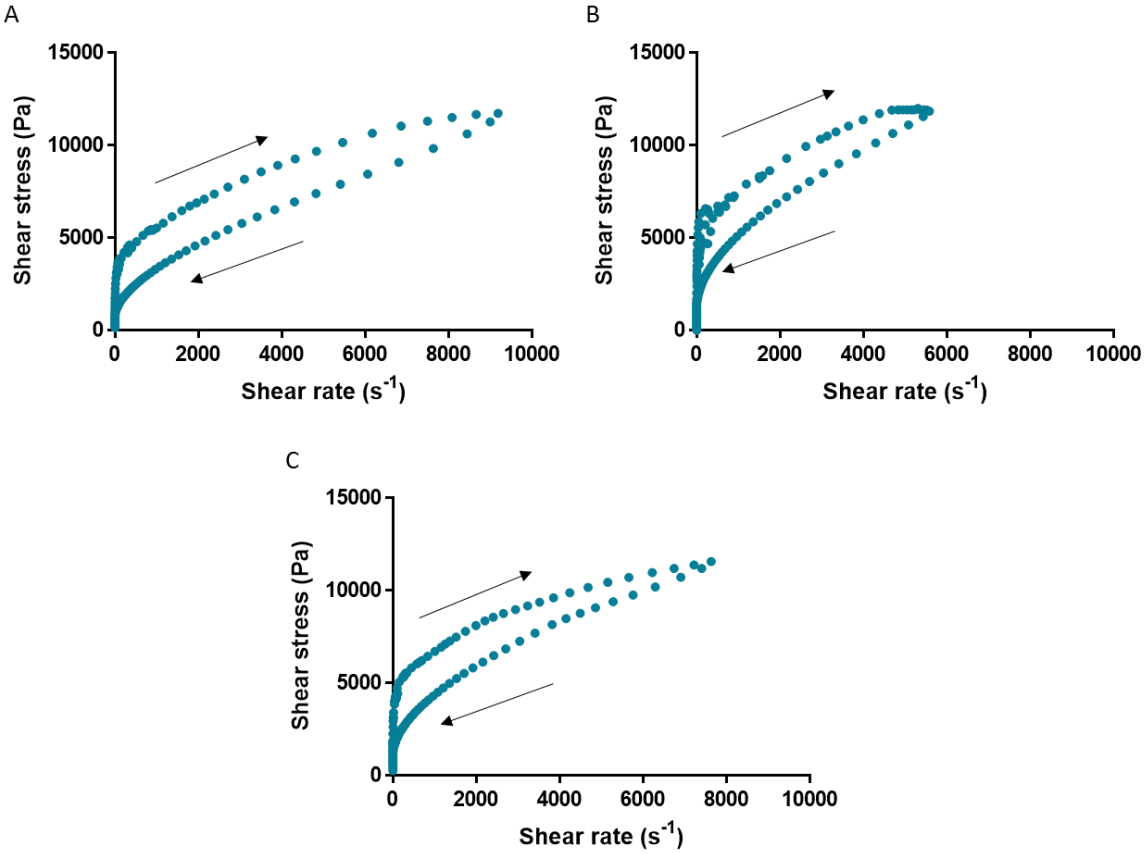

Figure 3.18 – Thixotropic behaviour of the NCC/glycerol gels with 7% NCC (w/w) (A - NCCs40', B - NCCs70' and C - NCCs130') assessed by the hysteresis loop experiment.

Due to the limitations described above, different shear rate windows were applied to the samples (as shown in figure 3.18, the maximum shear rate applied to the NCCs40' sample was ~10 000 s^{-1}, to the NCCs70' ~6000 s^{-1} and to the NCCs130' gel a maximum shear rate of ~8000 s^{-1} was applied). Nevertheless in order to be able to compare the three gels another set of test should have been done where the same shear rate window was selected, however due to time limitations it was not possible to repeat this study and only a qualitative result analyses was done. Despite of the encountered issue, each gel showed a well-defined hysteresis loop as described in the literature. [95][109] This indicates the recovery of the viscosity of the gels when the shear rate decreases along with the shear stress, which is a good indication of the thixotropy of the material referred in the literature.

To correlate the dependency of shear viscosity on the shear rate, shear viscosity and shear rate data retrieved from the hysteresis loop test are shown in figure 3.19. As expected, the shear viscosity of the samples decreases with the increase of shear rate. Before the linear decrease of the shear viscosity with the increase of the shear rate applied to the sample, is observed in every sample, an increase of the shear viscosity, which is characteristic of a typical flow curve of a viscous, shear thinning material. [110][111] No other conclusions can be infer from this figure, in particular the value of the yield strength for each gel cannot be considered due to the experimental parameters selected. In order to achieve the yield strength values, new curves should be plotted as describe above.

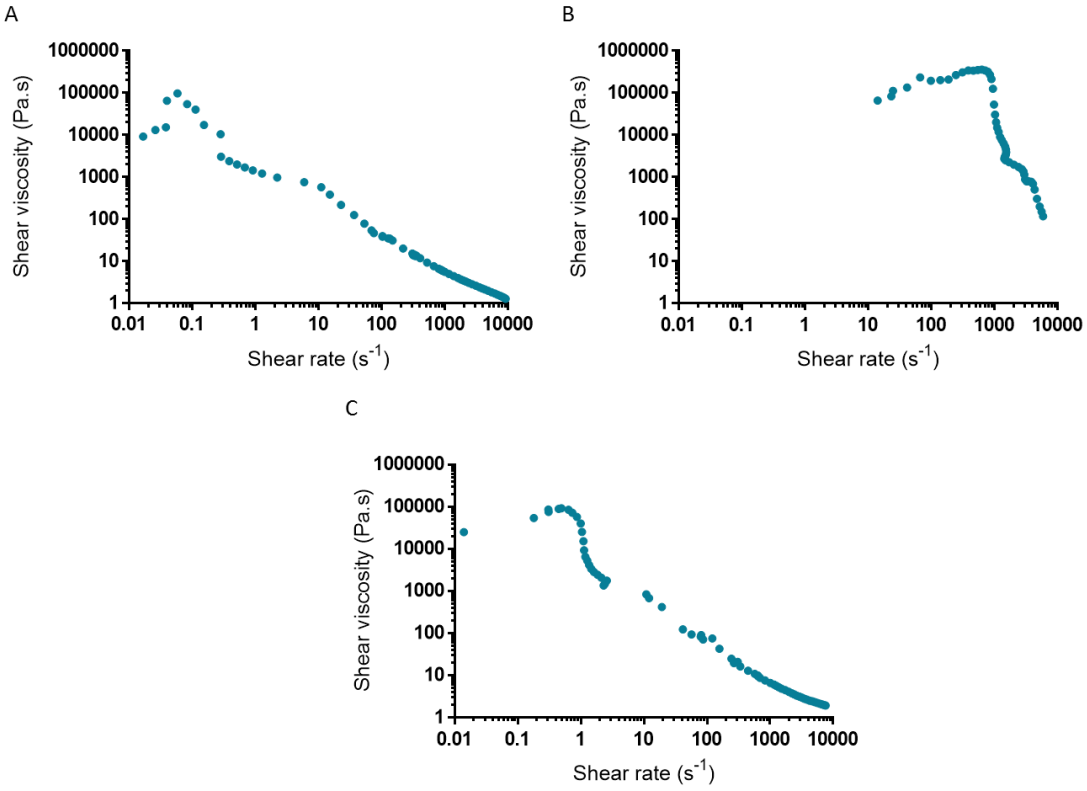

Figure 3.19 – Shear viscosity of the NCC/glycerol gels with 7% NCC (w/w) (A - NCCs40', B - NCCs70' and C - NCCs130') obtained from the shear rate ramps performed for the hysteresis loop tests.

4.3. Stress sweeps

In figure 3.20 are represented oscillatory stress sweeps. In this figure it can be seen an immediate partial recover of the initial more solid-like state of the gels, after the 4000 Pa shear stress ceased, which confirms the thixotropy properties reported in literature. [108] This transition is demonstrated by the phase angle values that increase to values higher than 45°, at a certain applied stress, when the gel is liquefied, and decreases to values below 45° when the LVR conditions start to be applied to the samples, occurring at the same time as the recovery of the gel.

Yield stress is the lower force (in this case, shear stress) applied to the material that is higher than the material's internal bonding forces. As of this stress, the material starts to flow and occurs a transition of the material from a solid-like state to a liquid-like state. [112] When the yield stress is achieved, *G'* starts to decrease and both *G"* and δ increase. [111] In table 3.8 the values of yield stress for each gel are stated and it seems that for higher NCC length (NCCs40'), the yield stress is higher (the gel starts to flow at a higher shear stress). However the values obtained for the three acid hydrolysis time are in the same order of magnitude.

From figure 3.20 it is observed that all the gels start to flow at low shear stresses (<70 Pa) however, the NCCs40' gels present a more liquid-like state at lower shear stress values than the remaining gels. As stated in the oscillatory frequency test, the overall behaviour of the NCCs70' and NCCs130' gel is quite similar. Both gels recover approximately 60% of their initial viscoelastic properties. However, the NCCs40' sample' can only recover 13% at the end of the test. A summary of these results is shown in table 3.8.

Table 3.8 – Summary of the properties of the NCC/glycerol gels with 7% NCC (w/w) (NCCs40', NCCs70' and NCCs130') retrieved from oscillatory stress sweep test followed by application of LVR conditions for 5 minutes.

Gels	Yield stress (Pa)	Transition solid-liquid stress (Pa)	Immediately Recover of after applying stress (%)	Maximum recover after solicitation (%)
NCCs40'	69.0	24.2e+02	7.5	13.0
NCCs70'	55.0	38.2e+02	52.6	64.6
NCCs130'	43.0	38.2e+02	54.7	64.7

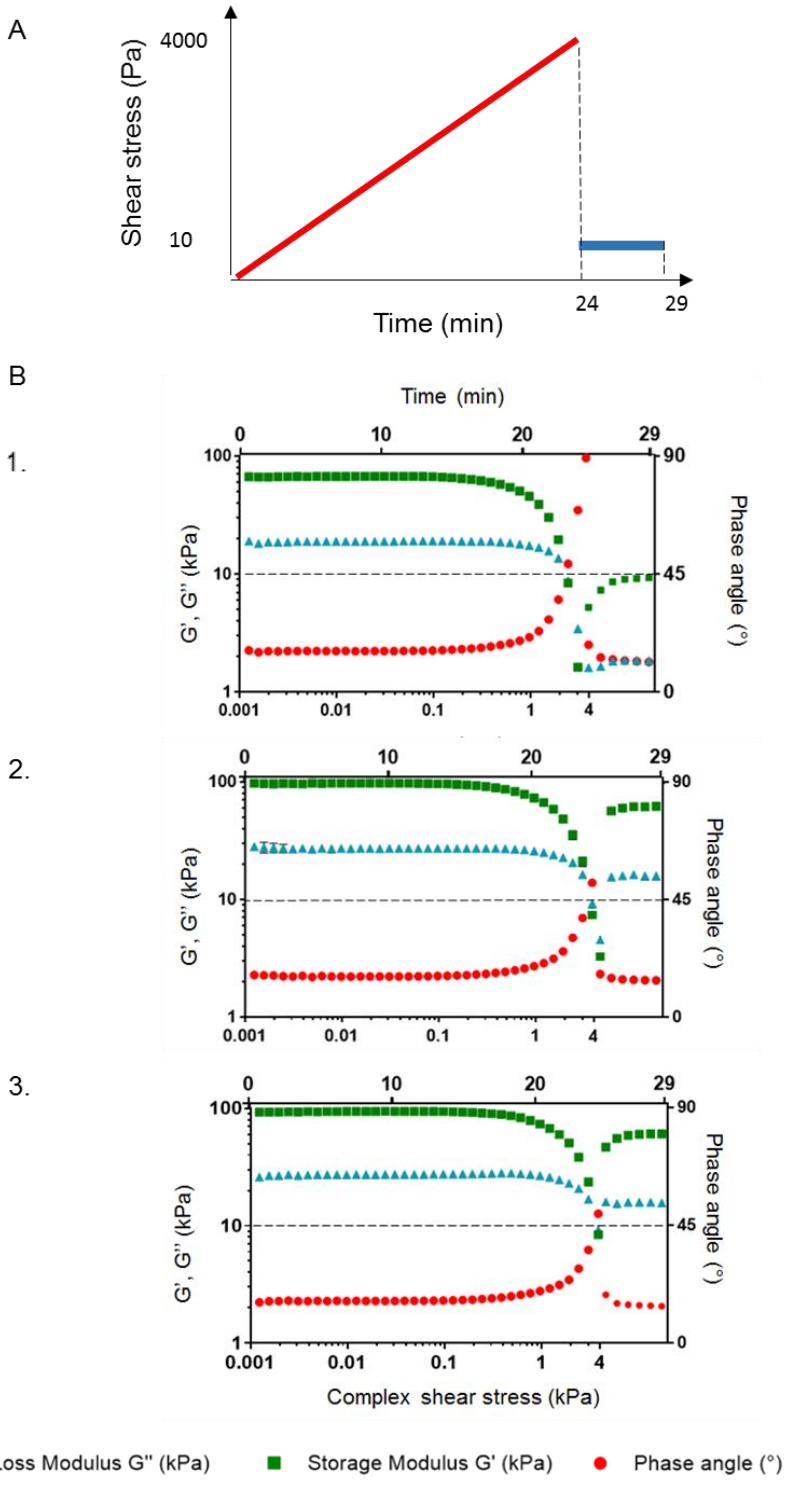

Figure 3.20 – A - Oscillatory stress sweep from 1 Pa to 4000 Pa followed by an application of the LVR conditions. B - Stress sweeps of the of the NCC/glycerol gels with 7% NCC (w/w) (1 - NCCs40', 2 - NCCs70' and 3 - NCCs130') at 2Hz, immediately followed by the application of a frequency and shear stress values within the LVR.

4.4. Additional rheological tests:

The sequence to assess the recovery capability of the gels consisted in an application of 4000 Pa in the gel for 1 minute, immediately followed by 4 minutes of application of the LVR frequency and stress conditions (2 Hz and 10 Pa, respectively). This test sequence was not executed properly by the rheometer. In each repetition of the sequence, the rheometer randomly decreased the value of the high shear stress applied. This sequence is represented in figure 3.21 and one can only use its data qualitatively.

Furthermore, from this figure, from the phase angle (δ) values, it is possible to conclude that the gels have the ability to constantly liquefy ($\delta > 45°$) at high shear stresses and posteriorly solidify when the LVR conditions are applied ($\delta < 45°$). This test also proves the thixotropic nature of the gels as well as its high capability to recover to its original solid state after a great number of solicitations.

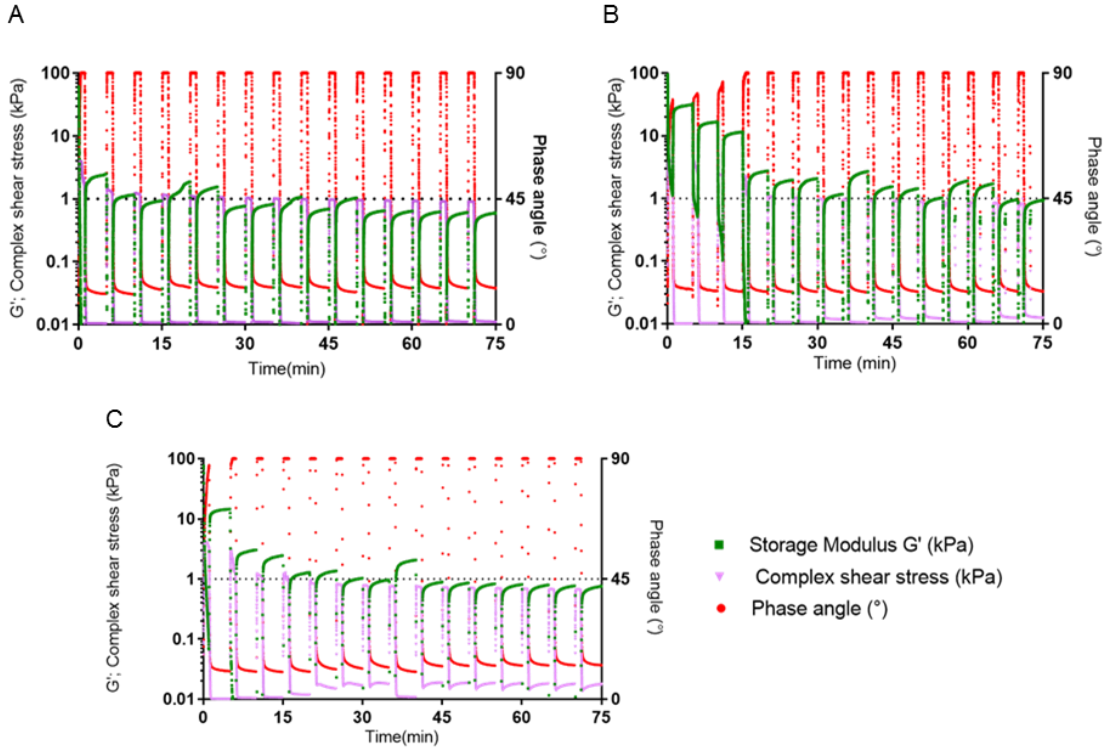

Figure 3.21 – Oscillating fixed stress of 4000 Pa at a 2Hz frequency applied for 1 minute followed by the application of the LVR conditions for 4 minutes The samples used are NCC/glycerol gels with 7% NCC (w/w) (A - NCCs40', B - NCCs70' and C - NCCs130').

After incubation in cell culture medium, a remarkable change in the physical properties of the gels was visually noticed. When attempting to manipulate the gels with a spatula they easily broke (Fig 3.22 - A). Due to this behaviour and in order to study the rheology of the gels, after this treatment they were prepared in disc casters (Fig 3.22 - B) and consequently, a smaller geometry plate (Ø 8 mm) was used. As the gels lose their thixotropic like properties after incubation in cell

culture medium, the oscillatory measurements were only performed with the NCCs40', to assess the viscoelastic properties of these gels as an example.

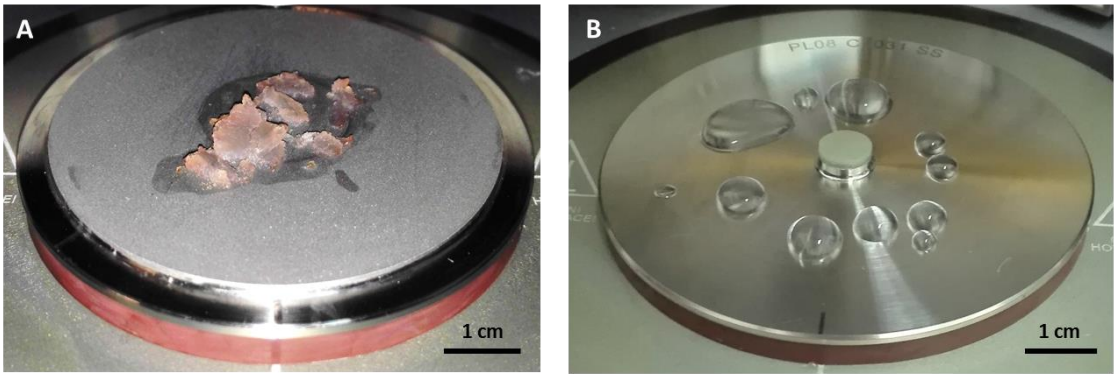

Figure 3.22 – Gels incubated in cell culture medium after the rheological measurements: A – Gel incubated and transferred from the well plate with a spatula; B – Gel prepared with the gel casters.

After the incubation with cell culture medium, the NCCs40' gel presented a more solid-like behaviour (Figure 3.23), with a *G'* higher than the *G''* and a phase angle below 45°.

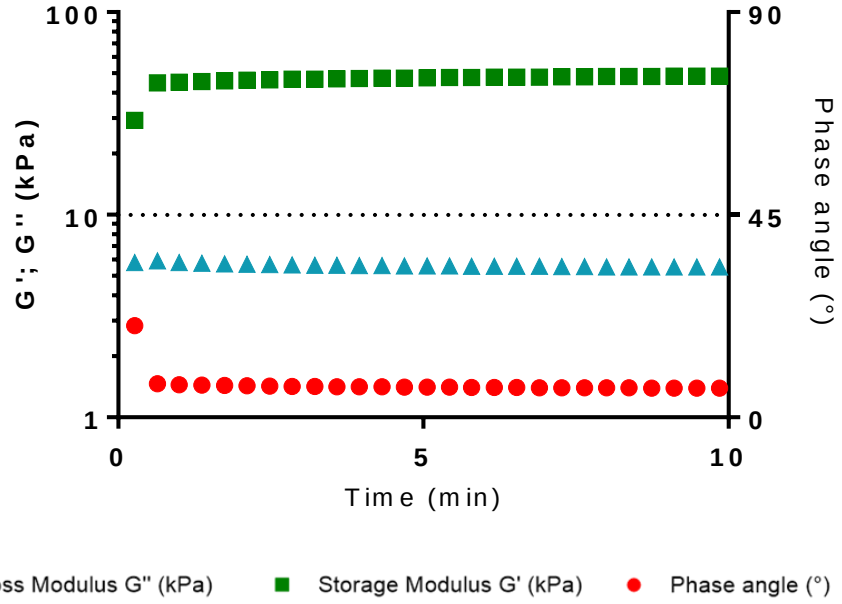

Figure 3.23 – Oscillation test of the NCCs40' gel after incubation with culture medium, with fixed shear stress and frequency values, both within the LVR of the NCCs40' gel (2 Hz, 10 Pa).

Comparing the loss and storage modulus and the phase angle of the NCCs40' gel incubated with cell culture medium with the dry NCCs40' gels (table 3.9), using the same values of frequency and shear stress, it is noticed a decrease in the loss modulus, and, consequently, in the phase angle, which value decreases to half. After the incubation with cell culture medium, the gels has a less liquid-like behaviour, which is in agreement with the previously referred brittleness.

These results can also be affected by the difference between the plate used in the rheological measurements of the gels without pH raise (Ø 20mm) and the plate used in the samples with pH of 8 (Ø 8mm). With the unforeseen fragility of the gel and the consequent necessity of the gel casters usage, there was no time to perform comparative rheological measurements with the gels without cell culture medium contact with an 8mm diameter plate.

Table 3.9 – Comparison of the viscoelastic properties of NCCs40' gel before and after incubation with cell culture medium.

Gels	*G'* (KPa)	*G''* (KPa)	Phase angle (°)
NCCs40' after incubation with cell culture medium	48.4 ± 17.3	5.5± 2.0	6.5 ± 0.2
NCCs40'	66.4 ± 9.8	18.6 ± 3.0	15.6 ± 0.9

From the studies shown, one could try to summarize a sort of relationship between the observed viscoelastic and thixotropy properties of the gels and its pitch. The gels containing the higher chiral nematic pitch (the NCCs40') are the gels that showed less capability to recover its initial viscoelastic properties, when compared to the gels with smaller chiral nematic pitches (NCCs70' and NCCs130').

5. Cell culture

5.1. Cell Adhesion:

In the figure 3.24 is represented the results from the cell adhesion test performed with NCC/glycerol gels.

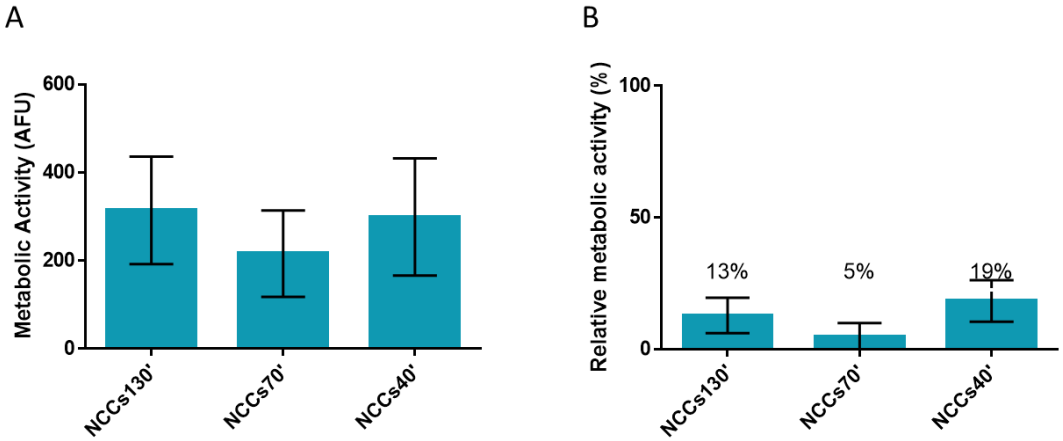

Figure 3.24 – Results from the 1st day of in vitro cell adhesion test for the NCCs130', NCCs70' and NCCs40'. A –Results from Resazurin fluorescence test. B – Relative cell viability graphic. Significance values were calculated by Mann-Whitney U test (p≤0.0001).

According to the results shown above, NCC/glycerol gels present a low cell adherence percentage. Despite these low values, further tests of cell proliferation and cell adhesion with longer incubation time should be performed. It is a possibility that these cells could proliferate and the material could still be suited for tissue engineering purposes with more extensive tests.

On the other hand, the low results of cell adhesion could be due to the negative surface charge of nanocrystalline cellulose (NCC) originated by the interaction of the hydroxyl groups of cellulose with the sulfate groups (-SO_3^--) resultant from the sulfuric acid hydrolysis and the negative zeta potential presented in this chapter. This reaction creates a negative electrostatic monolayer that repulses each NCC particle [113] and thus, the negatively charged cell membranes. Studies have shown that the negative charge of the NCC produced by sulfuric acid hydrolysis have repulsive effects in the internal integration of NCC in cells for bio imaging marking. [114] However, the negative charges of NCC can adsorb through electrostatic forces proteins or enzymes. [36] It was demonstrated by electro kinetic analysis that the NCC/glycerol gels surfaces have a negative zeta potential. The negative zeta potential is a factor that influences the cell adhesion process of fibroblasts along with another characteristics of the biomaterial. [115]

It is not possible to correlate the fingerprint texture size and the cell adhesion percentage. We can only verify that NCCs40'gel may have more weak points due to the gel formation that allows some cell adhesion.

5.2. Cytotoxicity assays:

In figure 3.25 are represented the graphics from the direct and indirect contact assays.

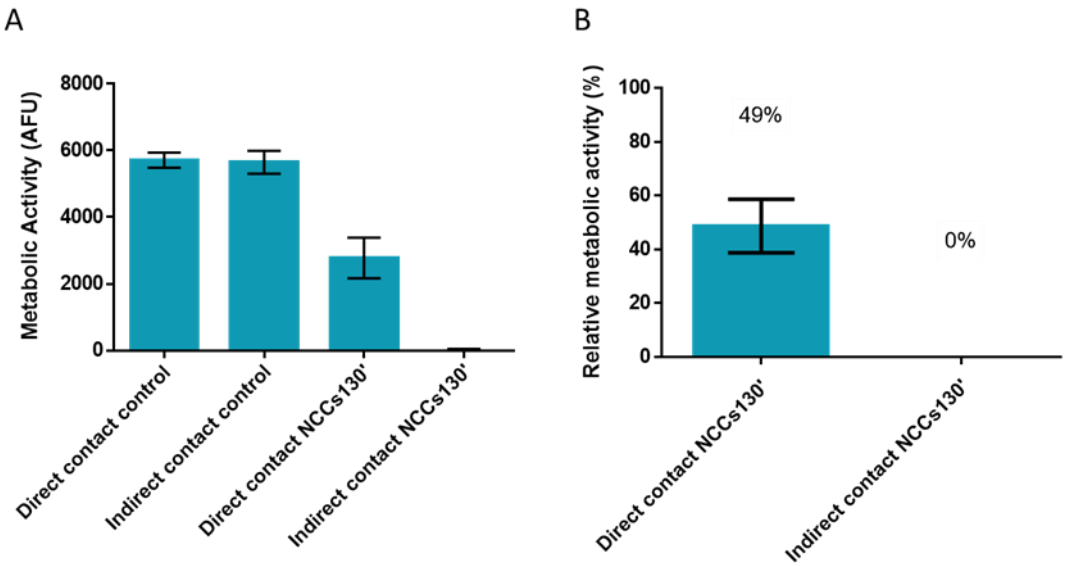

Figure 3.25 – Results from in vitro direct and indirect contact cytotoxicity assays for the NCCs130' gel. A – Results from Resazurin fluorescence test. B - Relative cell viability graphic. Significance values were calculated by Mann-Whitney U test (p≤0.0001).

As observed, there are no cells remaining in the indirect contact assay. This outcome could possibly be related to the release of cytotoxic compounds to the medium that were still present on the gel after the pH equilibrium procedure.

On the other hand, the results from the direct contact show a 49% of relative metabolic activity, which corroborates the hypothesis described above. The gel used in the direct contact did not had as many cytotoxic compounds as the culture medium, because the medium washed out those compounds, resulting in a significant relative metabolic activity percentage. With these outcomes, it is necessary to incubate the pH equilibrated gels for another 24 hours in culture medium before proceeding to cell culture.

Previous studies shown that NCC are not cytotoxic only when they are present in a concentration below 50 µg /ml in human endothelial cells [116] and 1000 µg/ml in NIH3T3 murine embryo fibroblast. [117] Although these studies show low cytotoxicity of NCC in contact with cells, they are not applicable to the gels in study, since the NCC concentration used in our work of 7% NCC/glycerol gels is 98000 µg/ml NCC in glycerol, that is very high when compared with the literature studies. The high concentration of NCC used, and the high content of sulphate groups present, can be associated with the decrease of the number of viable cells obtained in the direct and indirect contact test. However this hypothesis should be confirmed with complementing tests such as direct and indirect contact assays executed in gels with higher and lower percentage of NCC in their composition.

5.3. Final remarks:

Despite the cell adhesion tests showed a lower percentage of adherent cells, further tests should be performed. After the conclusions of the direct and indirect contact assays, the cell adhesion test should be repeated with 48 hours of gel incubation prior to any cell culture (24 hours for pH equilibrium as described in chapter II – section 4.3 plus 24 hours for the releasing of all the cytotoxic compounds that are still present within the gel). In addition, the period of the cell adhesion test should be longer, because the percentage of cell adhesion presented in the results could increase with time due to cell growth and expansion. The results shown in section 5.1 are not sufficient to categorize the NCC/glycerol gels as a non-fouling material.

Furthermore, cell proliferation tests should also be executed for further information in the viability of the gels for tissue engineering purposes.

6. Collagen gels

Gelation of collagen was not observed and no further tries were performed due to shortage of time.

Collagen in acetic acid was placed in an ammoniac vapour chamber for a month and the process was repeated one more time. Gelation was never observed.

A possible reason for this outcome can be attributed to structural and chemical differences between Achilles bovine tendon collagen (used in this work) and rat tail collagen (used by other authors). For instance, dehydrated fibrils of rat tail collagen have a Young modulus of 11 GPa [118] and the achilles bovine tendon have a 5 GPa Young modulus. [119] Cross-linked scaffolds of rat tail tendon and achilles bovine tendon type I collagen also showed that fibroblasts preferentially bind to the collagen scaffold from the rat tail tendon. [120] Furthermore, amino acid differences were detected in equine and bovine collagen. The conclusion of the study conducted by Angele et al., stated that tissue engineering data acquired from a collagen of a certain animal species may not be transferable to scaffolds constituted by a different animal source of collagen due to differences in the physico-chemical properties of the collagens. [121]

Chapter IV - Conclusion

The aim of this study was to obtained gels with liquid crystalline phases and investigates the relationship between the liquid crystalline phases, mainly, chiral nematic and the cell behaviour when in contact with these conformations. Also, the evaluation of the material's behaviour when in contact with cell culture was a subject of interest.

To conduct this research, three environments were considered: collagen, NCC/glycerol and NCC/PVA gels. NCC and collagen were chosen due to its possibility to self-assemble into a liquid crystalline phase. Production of NCC with 40 min, 70 min and 130 min sulfuric acid hydrolysis times were set in an attempt to evaluate the relationship between liquid crystalline textures and NCC length. Through SEM, NCC's width and length were measured.

Gelation of type I collagen of achilles bovine tendon did not occur as expected from the adapted protocol, possibly due to the chemical and structural difference between the bovine Achilles tendon type I collagen used in this study and the rat tail tendon type I collagen used in the procedure from literature. NCC/PVA gelation was successfully achieved, however the NCC/PVA hydrogels did not present liquid crystalline texture either in TEM and POM analysis and hence no further studies were conducted with these gels. NCC/glycerol gels were successfully produced and present the characteristic textures observed in the NCC chiral nematic liquid crystalline phase.

The first method used to confirm the liquid crystalline phases was analyse its optical properties with POM, where fingerprint textures in NCC/glycerol gels were visualized and only birefringence was observed in NCC/PVA hydrogels. Different concentrations of NCC in the gels were compared and alterations in the pitch of the "fingerprint" texture measured. Also the effect of different acid hydrolysis time, and hence different lengths, was evaluated. The pitch of the fingerprint texture was estimated to be around 4-16 μm and increases with the NCC length. Initial integrity tests showed the ability of the gel to swell PBS into its matrix. Due to the presence of the fingerprint texture in the 7% (w/w) NCC concentration in the gels, this concentration was selected in the subsequent studies. Parallel to these studies, and using the same concentration, NCC with different sulfuric acid hydrolysis time were used in the gels to evaluate the influence of the NCC length in the gels properties.

To prepare the NCC/glycerol gels for the cell culture, a rise of the pH to 8 of the gels was achieved successfully both with PBS and cell culture medium. To ensure the preservation of the liquid crystalline texture in the gels, new observations with POM were done prior to cell culture. The gels, after the rise of pH, maintained the fingerprint texture and when culture medium was used to raise the pH, was noted an increase of the pitch of the" fingerprint" texture of the gels. EKA results showed that the gels have a negative zeta potential (> -10 mV). Rheological studies confirmed the thixotropy of the gels with a dominance of the elastic component, *G'*, in LVR conditions. Gels with NCC obtained with 40 min of acid hydrolysis showed less elastic properties

than the ones obtained with longer times. A decrease in the viscous component of the material and the conservation of the elastic component dominance was also examined in gels after 48 hours of incubation with culture medium.

Indirect and direct contact assays showed that cytotoxic compounds were still released from the gels after 48 hours of incubation in cell culture medium. In the indirect contact assay, no cells survived. On the contrary, direct contact 49% of cell survival which led to state conclude that a 48 hour minimum time of pH equilibrium is necessary before initiate cell culture. Adhesion tests showed that the percentage of adhere cells is low (5%-19% of cell adhesion) but further tests should be performed to conclude if the material is non-fouling or is still suitable for tissue engineering purposes.

From the results described above it can be concluded that the liquid crystalline NCC/glycerol gels present interesting features: i) additionally to their thixotropy property, the gels can recover from liquid to solid state after several cycles of solicitation; ii) the increase of the gels' pH, required to work with the fibroblast cells, does not seem to affect the liquid crystalline features of the gel; iii) the gels showed low cytotoxicity after 48 hours of incubation (24h from the pH raise plus 24h of incubation in the direct contact test) iv) although the preliminary cell studies demonstrate low cell adhesion (obtained with 24h of cell medium incubation time), the application of 48h of incubation with culture medium prior to cell culture and the realization of proliferation and more extensive cell adhesion studies could lead to a good cytotoxic response.

Despite the fact that further studies should be done in order to establish the biocompatibility nature of the liquid crystalline NCC/glycerol gels the results presented here already show a promising material to be applied in the tissue engineering field.

Chapter V - Future directions

NCC/glycerol gels are far from being totally characterized and studied. Further chemical and physical characterization studies should be perform. Supplementary proliferation and cell adhesion tests should also be completed in order to evaluate the viability of the gel for tissue engineering applications and confirm/disprove the non-fouling nature of the material.

Further rheological studies at 37°C as well as quantitative viscosity assays and other complementary rheological tests should be conducted for a fully understanding of the thixotropic properties of these materials. The capability of the NCC/glycerol gels to recover from a liquid state to a solid state after a solicitation (thixotropy) could lead to the appliance of this gels as injectable biomaterials for bone, tendon and muscle regeneration (due to the gels liquid crystal conformation similar of these biological structures).

If the materials proves to be non-fouling, chemically modification of the NCC surface or NCC/glycerol gels can be a viable path to develop a scaffold for tissue engineering, Many studies were performed to functionalize or chemically alter the NCC surface. Future studies should emphasis the RGD functionalization of NCC to enhance cell adhesion. This functionalization was already done in bacterial cellulose, which was modified with xyloglucan and RGD to adhere epithelial cells. [122] Bacterial nanocellulose (BNC) scaffolds were functionalized with type I collagen and fibronectin to enhance the cell adhesion of the material [123]. Other alternative to induce cell adhesion is the surface coating of the material with positive charged polyelectrolyte PAHCL. This method was used in adhesion and growth of C2C12 myoblasts in functionalized NCC. [124]

Interactions of the NCC/glycerol gels with proteins is another field yet to be explored. Functionalized nanocellulose, such as nano fibrillated cellulose has successfully bounded proteins [125] and is able to bound to specific Human IgG [126]. On the other hand, NCC functionalized with gold nanoparticles are successfully used as a matrix for CGTase enzyme immobilization [127] as well as for the enzyme glucose oxidase [128].

Further studies to understand if the pitch of the NCC/glycerol gels is tunable in certain conditions, such as when in presence of an electric or magnetic field would be very interesting and could lead to new developments in electronics as well as in creation of new (bio) sensors [129].

NCC already showed photonic properties that could also be explored in the future [130].

In conclusion, NCC/glycerol gels have an enormous potential in a variety of fields and there has to be conducted additional studies and exploration of these potentialities.

References:

[1] Y. Bouligand, “Liquid crystals and biological morphogenesis: Ancient and new questions”, *Comptes Rendus Chim.*, vol. 11, pp. 281–296, 2008.

[2] Y.-Y. Luk, S. F. Campbell, N. L. Abbott, and C. J. Murphy, “Non-toxic thermotropic liquid crystals for use with mammalian cells”, *Liq. Cryst.*, vol. 31, no. October 2014, pp. 611–621, 2004.

[3] L. Besseau, B. Coulomb, C. Lebreton-Decoster, and M. M. Giraud-Guille, “Production of ordered collagen matrices for three-dimensional cell culture”, *Biomaterials*, vol. 23, pp. 27–36, 2002.

[4] R. J. Carlton, J. T. Hunter, D. S. Miller, R. Abbasi, P. C. Mushenheim, L. N. Tan, and N. L. Abbott, “Chemical and biological sensing using liquid crystals.”, *Liq. Cryst. Rev.*, vol. 1, no. January 2015, pp. 29–51, 2013.

[5] X. Dong, J. Revol, and D. Gray, “Effect of microcrystallite preparation conditions on the formation of colloid crystals of cellulose”, *Cellulose*, vol. 5, no. 1, pp. 19–32, 1998.

[6] C. Guo, J. Wang, F. Cao, R. J. Lee, and G. Zhai, “Lyotropic liquid crystal systems in drug delivery”, *Drug Discov. Today*, vol. 15, no. 23–24, pp. 1032–1040, 2010.

[7] T. Ikeda, T. Sasaki, and K. Ichimura, “Photochemical switching of polarization in ferroelectric liquid-crystal films”, *Nature*, vol. 361, pp. 428–430, 1993.

[8] D. Demus, J. Goodby, G. Gray, H. Spiess, and V. Vill, *Handbook of Liquid Crystals, Vol.1 Fundamentals*. Weinheim: WILEY - VCH, 1998.

[9] G. H. Brown and J. J. Wolken, *Liquid Crystals and Biological Structures*. London: Academic Press, 1979.

[10] H. Uehara and J. Hatano, “Pressure-Temperature Phase Diagrams of Ferroelectric Liquid Crystals”, *J. Phys. Soc. Japan*, vol. 71, no. 2, pp. 509–512, 2002.

[11] S. J. Woltman, G. D. Jay, and G. P. Crawford, “Liquid-crystal materials find a new order in biomedical applications.”, *Nat. Mater.*, vol. 6, pp. 929–938, 2007.

[12] M. M. Giraud-Guille, “Liquid crystalline order of biopolymers in cuticles and bones.”, *Microsc. Res. Tech.*, vol. 27, pp. 420–428, 1994.

[13] Y. K. Murugesan and A. D. Rey, “Modeling textural processes during self-assembly of plant-based chiral-nematic liquid crystals”, *Polymers (Basel).*, vol. 2, pp. 766–785, 2010.

[14] K. Hiltrop, “Phase Chirality of Micellar Lyotropic Liquid Crystals”, *Liq. Cryst.*, pp. 447–480.

[15] A. D. Rey, “Liquid crystal models of biological materials and processes”, *Soft Matter*, vol. 6, p. 3402, 2010.

[16] R. Martin, J. Farjanel, D. Eichenberger, a Colige, E. Kessler, D. J. Hulmes, and M. M. Giraud-Guille, “Liquid crystalline ordering of procollagen as a determinant of three-dimensional extracellular matrix architecture.”, *J. Mol. Biol.*, vol. 301, pp. 11–17, 2000.

[17] M. M. Giraud-Guille, G. Mosser, and E. Belamie, “Liquid crystallinity in collagen systems in vitro and in vivo”, *Curr. Opin. Colloid Interface Sci.*, vol. 13, pp. 303–313, 2008.

[18] E. Belamie, G. Mosser, F. Gobeaux, and M. M. Giraud-Guille, “Possible transient liquid crystal phase during the laying out of connective tissues: α-chitin and collagen as models”, *J. Phys. Condens. Matter*, vol. 18, pp. S115–S129, 2006.

[19] D. G. Gray, “Chiral nematic ordering of polysaccharides”, *Carbohydr. Polym.*, vol. 25, no. 1994, pp. 277–284, 1994.

[20] M.-M. Giraud-Guille, E. Belamie, G. Mosser, C. Helary, F. Gobeaux, and S. Vigier, “Liquid crystalline properties of type I collagen: Perspectives in tissue morphogenesis”, *Comptes Rendus Chim.*, vol. 11, pp. 245–252, 2008.

[21] C. Blanc, D. Coursault, and E. Lacaze, “Ordering nano- and microparticles assemblies

with liquid crystals", *Liq. Cryst. Rev.*, vol. 1, no. January 2015, pp. 83–109, 2013.

[22] A. D. Rey, E. Herrera-Valencia, and Y. K. Murugesan, "Structure and dynamics of biological liquid crystals", *Liq. Cryst.*, vol. 41, no. January 2015, pp. 430–451, 2014.

[23] L. T. De Haan, J. M. N. Verjans, D. J. Broer, C. W. M. Bastiaansen, and A. P. H. J. Schenning, "Humidity-responsive liquid crystalline polymer actuators with an asymmetry in the molecular trigger that bend, fold, and curl", *J. Am. Chem. Soc.*, vol. 136, pp. 10585–10588, 2014.

[24] I. Lin, D. Miller, P. Bertics, C. Murphy, J. Pablo, and N. Abbott, "Endotoxin-Induced Structural Transformations in Liquid Crystalline Droplets", *Science*, vol. 332, no. 6035, pp. 997–1003, 2011.

[25] J. M. Brake and N. L. Abbott, "An experimental system for imaging the reversible adsorption of amphiphiles at aqueous-liquid crystal interfaces", *Langmuir*, vol. 18, no. 11, pp. 6101–6109, 2002.

[26] J. E. Kirkwood and G. G. Fuller, "Liquid crystalline collagen: A self-assembled morphology for the orientation of mammalian cells", *Langmuir*, vol. 25, no. 17, pp. 3200–3206, 2009.

[27] M. M. Giraud Guille, G. Mosser, C. Helary, and D. Eglin, "Bone matrix like assemblies of collagen: From liquid crystals to gels and biomimetic materials", *Micron*, vol. 36, pp. 602–608, 2005.

[28] A. Yaari, Y. Posen, and O. Shoseyov, "Liquid crystalline human recombinant collagen: the challenge and the opportunity.", *Tissue Eng. Part A*, vol. 19, pp. 1502–6, 2013.

[29] W. J. Chung, A. Merzlyak, S. Y. Yoo, and S. W. Lee, "Genetically engineered liquid-crystalline viral films for directing neural cell growth", *Langmuir*, vol. 26, no. 17, pp. 9885–9890, 2010.

[30] J. Bender, M. B. Ericson, N. Merclin, V. Iani, A. Rosén, S. Engström, and J. Moan, "Lipid cubic phases for improved topical drug delivery in photodynamic therapy", *J. Control. Release*, vol. 106, no. 3, pp. 350–360, 2005.

[31] D. Klemm, B. Heublein, H. P. Fink, and A. Bohn, "Cellulose: Fascinating biopolymer and sustainable raw material", *Angew. Chemie - Int. Ed.*, vol. 44, pp. 3358–3393, 2005.

[32] R. M. a Domingues, M. E. Gomes, and R. L. Reis, "The potential of cellulose nanocrystals in tissue engineering strategies", *Biomacromolecules*, vol. 15, pp. 2327–2346, 2014.

[33] D. Klemm, F. Kramer, S. Moritz, T. Lindström, M. Ankerfors, D. Gray, and A. Dorris, "Nanocelluloses: A new family of nature-based materials", *Angew. Chemie - Int. Ed.*, vol. 50, pp. 5438–5466, 2011.

[34] B. L. Peng, N. Dhar, H. L. Liu, and K. C. Tam, "Chemistry and applications of nanocrystalline cellulose and its derivatives: A nanotechnology perspective", *Can. J. Chem. Eng.*, vol. 89, no. October, pp. 1191–1206, 2011.

[35] J.-F. Revol, L. Godbout, X.-M. Dong, D. G. Gray, H. Chanzy, and G. Maret, "Chiral nematic suspensions of cellulose crystallites; phase separation and magnetic field orientation", *Liq. Cryst.*, vol. 16, no. May 2013, pp. 127–134, 1994.

[36] N. Lin and A. Dufresne, "Nanocellulose in biomedicine: Current status and future prospect", *Eur. Polym. J.*, vol. 59, pp. 302–325, 2014.

[37] X. Yang, E. Bakaic, T. Hoare, and E. D. Cranston, "Injectable polysaccharide hydrogels reinforced with cellulose nanocrystals: Morphology, rheology, degradation, and cytotoxicity", *Biomacromolecules*, vol. 14, pp. 4447–4455, 2013.

[38] H. E. Kaufman, T. L. Steinemann, E. Lehman, H. W. Thompson, E. D. Varnell, J. T. Jacob-LaBarre, and B. M. Gebhardt, "Collagen-based drug delivery and artificial tears.", *J. Ocul. Pharmacol.*, vol. 10, no. 1, pp. 17–27, 1994.

[39] K. Manish and K. G. T., "Recent advances in opthalmic drug delivery system", *Int. J. Pharm. Pharm. Sci.*, vol. 4, no. 1, pp. 387–394, 2012.

[40] K. Panduranga Rao, “Recent developments of collagen-based materials for medical applications and drug delivery systems”, *J. Biomater. Sci. Polym. Ed.*, vol. 7, no. 7, pp. 623–645, 1996.

[41] D. Stopak, N. K. Wessells, and a K. Harris, “Morphogenetic rearrangement of injected collagen in developing chicken limb buds.”, *Proc. Natl. Acad. Sci. U. S. A.*, vol. 82, no. May, pp. 2804–2808, 1985.

[42] T. Kofidis, P. Akhyari, J. Boublik, P. Theodorou, U. Martin, a. Ruhparwar, S. Fischer, T. Eschenhagen, H. P. Kubis, T. Kraft, R. Leyh, and a. Haverich, “In vitro engineering of heart muscle: Artificial myocardial tissue”, *J. Thorac. Cardiovasc. Surg.*, vol. 124, no. 1, pp. 63–69, 2002.

[43] C. H. Lee, A. Singla, and Y. Lee, “Biomedical applications of collagen”, *Int. J. Pharm.*, vol. 221, pp. 1–22, 2001.

[44] N. M. Sangeetha and U. Maitra, “Supramolecular gels: functions and uses.”, *Chem. Soc. Rev.*, vol. 34, pp. 821–836, 2005.

[45] T. Kato, Y. Hirai, S. Nakaso, and M. Moriyama, “Liquid-crystalline physical gels.”, *Chem. Soc. Rev.*, vol. 36, no. 12, pp. 1857–1867, 2007.

[46] N. Mizoshita, Y. Suzuki, K. Kishimoto, K. Hanabusa, and T. Kato, “Electrooptical properties of liquid-crystalline physical gels: a new oligo(amino acid) gelator for light scattering display materials”, *J. Mater. Chem.*, vol. 12, pp. 2197–2201, 2002.

[47] N. Annabi, A. Tamayol, J. A. Uquillas, M. Akbari, L. E. Bertassoni, C. Cha, G. Camci-Unal, M. R. Dokmeci, N. a. Peppas, and A. Khademhosseini, “25th anniversary article: Rational design and applications of hydrogels in regenerative medicine”, *Adv. Mater.*, vol. 26, pp. 85–124, 2014.

[48] A. S. Hoffman, “Hydrogels for biomedical applications”, *Adv. Drug Deliv. Rev.*, vol. 64, pp. 18–23, 2012.

[49] B. D. Ratner, A. S. Hoffman, F. J. Schoen, and J. E. Lemons, *Biomaterials Science: An Introduction to Materials in Medicine*. New York: Elsevier, 2004.

[50] E. M. Ahmed, “Hydrogel: Preparation, characterization, and applications”, *J. Adv. Res.*, 2013.

[51] S. S. Nair, J. Y. Zhu, Y. Deng, and A. J. Ragauskas, “Hydrogels Prepared from Cross-Linked Nano fi brillated Cellulose”, 2014.

[52] Z. Hu, E. D. Cranston, R. Ng, and R. Pelton, “Tuning cellulose nanocrystal gelation with polysaccharides and surfactants.”, *Langmuir*, vol. 30, pp. 2684–92, 2014.

[53] C. Helary, I. Bataille, A. Abed, C. Illoul, A. Anglo, L. Louedec, D. Letourneur, A. Meddahi-Pellé, and M. M. Giraud-Guille, “Concentrated collagen hydrogels as dermal substitutes”, *Biomaterials*, vol. 31, no. 3, pp. 481–490, 2010.

[54] H. Betre, S. R. Ong, F. Guilak, A. Chilkoti, B. Fermor, and L. a. Setton, “Chondrocytic differentiation of human adipose-derived adult stem cells in elastin-like polypeptide”, *Biomaterials*, vol. 27, pp. 91–99, 2006.

[55] H. Betre, L. a. Setton, D. E. Meyer, and A. Chilkoti, “Characterization of a genetically engineered elastin-like polypeptide for cartilaginous tissue repair”, *Biomacromolecules*, vol. 3, no. 1, pp. 910–916, 2002.

[56] A. Mihranyan, “Viscoelastic properties of cross-linked polyvinyl alcohol and surface-oxidized cellulose whisker hydrogels”, *Cellulose*, vol. 20, no. 3, pp. 1369–1376, 2013.

[57] N. a. Peppas and N. K. Mongia, “Ultrapure poly(vinyl alcohol) hydrogels with mucoadhesive drug delivery characteristics”, *Eur. J. Pharm. Biopharm.*, vol. 43, no. 1, pp. 51–58, 1997.

[58] T. Abitbol, T. Johnstone, T. M. Quinn, and D. G. Gray, “Reinforcement with cellulose nanocrystals of poly(vinyl alcohol) hydrogels prepared by cyclic freezing and thawing”, *Soft Matter*, vol. 7, no. 6, p. 2373, 2011.

[59] B. Schyrr, S. Pasche, G. Voirin, C. Weder, Y. C. Simon, and E. J. Foster, “Biosensors Based on Porous Cellulose Nanocrystal-Poly(vinyl Alcohol) Scaffolds.”, *ACS Appl. Mater. Interfaces*, 2014.

[60] J. S. Gonzalez, L. N. Ludueña, A. Ponce, and V. a. Alvarez, “Poly(vinyl alcohol)/cellulose nanowhiskers nanocomposite hydrogels for potential wound dressings”, *Mater. Sci. Eng. C*, vol. 34, no. 1, pp. 54–61, 2014.

[61] K. C. Dee, D. Puleo, and R. Bizios, *Tissue- Biomaterial Interactions*, 1st ed. New Jersey: Wiley-Liss, 2002.

[62] A. Hoffman, “Non-fouling surface technologies.”, *J. Biomater. Sci. Polym. Ed.*, vol. 10, no. 10, pp. 1011–1014, 1999.

[63] S. Chen and S. Jiang, “A new avenue to nonfouling materials”, *Adv. Mater.*, vol. 20, no. 2, pp. 335–338, 2008.

[64] L. Richert, F. Boulmedais, P. Lavalle, J. Mutterer, E. Ferreux, G. Decher, P. Schaaf, J.-C. Voegel, and C. Picart, “Improvement of stability and cell adhesion properties of polyelectrolyte multilayer films by chemical cross-linking.”, *Biomacromolecules*, vol. 5, no. 2, pp. 284–94, 2004.

[65] A. Hansson, N. Hashom, F. Falson, P. Rousselle, O. Jordan, and G. Borchard, “In vitro evaluation of an RGD-functionalized chitosan derivative for enhanced cell adhesion”, *Carbohydr. Polym.*, vol. 90, no. 4, pp. 1494–1500, 2012.

[66] S. Corda, J. L. Samuel, and L. Rappaport, “Extracellular matrix and growth factors during heart growth”, *Heart Fail. Rev.*, vol. 5, no. 2, pp. 119–130, 2000.

[67] B. E. a. Alberts, *Molecular Biology of The Cell*, vol. 4. NCBI - PUBMED, 2002.

[68] R. Kalluri and M. Zeisberg, “Fibroblasts in cancer”, *Nat. Rev. Cancer*, vol. 6, no. 5, pp. 392–401, 2006.

[69] L. Healy and L. Ruban, *Atlas of Human Pluripotent Stem Cells*, New York: Springer, 2012.

[70] P. Camelliti, T. K. Borg, and P. Kohl, “Structural and functional characterisation of cardiac fibroblasts”, *Cardiovasc. Res.*, vol. 65, no. 1, pp. 40–51, 2005.

[71] M. Iwano, D. Plieth, T. M. Danoff, C. Xue, H. Okada, and E. G. Neilson, “Evidence that fibroblasts derive from epithelium during tissue fibrosis”, vol. 110, no. 3, pp. 305–306, 2002.

[72] S. G. Guerreiro, M. J. Oliveira, M. a. Barbosa, R. Soares, and P. L. Granja, “Neonatal human dermal fibroblasts immobilized in RGD-alginate induce angiogenesis”, *Cell Transplant.*, vol. 23, no. 8, pp. 945–957, 2014.

[73] Y. Changa, H. Li, and Z. Guob, “Mesenchymal Stem Cell-Like Properties in Fibroblasts”, *Cell. Physiol. Biochem.*, vol. 34, no. 601, pp. 703–714, 2014.

[74] A. Takashima, “Establishment of fibroblast cultures”, *Curr. Protoc. Cell Biol.*, vol. Chapter 2, p. Unit 2.1, 1998.

[75] T. Tischer, S. Vogt, S. Aryee, E. Steinhauser, C. Adamczyk, S. Milz, V. Martinek, and A. B. Imhoff, “Tissue engineering of the anterior cruciate ligament: A new method using acellularized tendon allografts and autologous fibroblasts”, *Arch. Orthop. Trauma Surg.*, vol. 127, no. 9, pp. 735–741, 2007.

[76] R. a. Weiss, M. a. Weiss, K. L. Beasley, and G. Munavalli, “Autologous cultured fibroblast injection for facial contour deformities: A prospective, placebo-controlled, phase III clinical trial”, *Dermatologic Surg.*, vol. 33, no. 3, pp. 263–268, 2007.

[77] N. Yamada, N. Shioya, and Y. Kuroyanagi, “Evaluation of an allogeneic cultured dermal substitute composed of fibroblasts within a spongy collagen matrix as a wound dressing.”, *Scand. J. Plast. Reconstr. Surg. Hand Surg.*, vol. 29, no. 3, pp. 211–219, 1995.

[78] H. Parmar, P. Young, J. T. Emerman, R. M. Neve, S. Dairkee, and G. R. Cunha, “A novel method for growing human breast epithelium in vivo using mouse and human mammary

fibroblasts", *Endocrinology*, vol. 143, no. 12, pp. 4886–4896, 2002.

[79] W. Marston, J. Hanft, P. Norwood, and R. Pollak, "The Efficacy and Safety of Dermagraft in Improving the Healing of Chronic Diabetic Foot Ulcers", *Diabetes Care*, vol. 26, no. 6, pp. 1701–1705, 2003.

[80] R. S. Kirsner, W. a Marston, R. J. Snyder, T. D. Lee, D. I. Cargill, and H. B. Slade, "Spray-applied cell therapy with human allogeneic fibroblasts and keratinocytes for the treatment of chronic venous leg ulcers: a phase 2, multicentre, double-blind, randomised, placebo-controlled trial", *Lancet*, vol. 380, no. 9846, pp. 977–985, 2012.

[81] Z. H. Syedain, L. a. Meier, J. W. Bjork, A. Lee, and R. T. Tranquillo, "Implantable arterial grafts from human fibroblasts and fibrin using a multi-graft pulsed flow-stretch bioreactor with noninvasive strength monitoring", *Biomaterials*, vol. 32, no. 3, pp. 714–722, 2011.

[82] C. Choong, D. Hutmacher, and J. Triffitt, "Co-culture of Bone Marrow Fibroblasts and Endothelial Cells on Modified Polycaprolactone Substrates for Enhanced Potentials in Bone Tissue Engineering", *Tissue Eng.*, vol. 12, no. 9, 2006.

[83] W.-J. Chung, A. Merzlyak, and S.-W. Lee, "Fabrication of engineered M13 bacteriophages into liquid crystalline films and fibers for directional growth and encapsulation of fibroblasts", *Soft Matter*, vol. 6, no. 18, p. 4454, 2010.

[84] J. F. Revol, H. Bradford, J. Giasson, R. H. Marchessault, and D. G. Gray, "Helicoidal self-ordering of cellulose microfibrils in aqueous suspension.", *Int. J. Biol. Macromol.*, vol. 14, no. 3, pp. 170–172, 1992.

[85] E. D. Cranston and D. G. Gray, "Morphological and optical characterization of polyelectrolyte multilayers incorporating nanocrystalline cellulose", *Biomacromolecules*, vol. 7, pp. 2522–2530, 2006.

[86] W. J. Orts, J. Shey, S. H. Imam, G. M. Glenn, M. E. Guttman, and J. F. Revol, "Application of cellulose microfibrils in polymer nanocomposites", *J. Polym. Environ.*, vol. 13, no. 4, pp. 301–306, 2005.

[87] A. Dorris and D. G. Gray, "Gelation of cellulose nanocrystal suspensions in glycerol", *Cellulose*, vol. 19, pp. 687–694, 2012.

[88] K. Kalantar-Zadeh and B. Fry, *Nanotechnology-enabled sensors*. New York: Springer, 2008.

[89] I. Dierking, *Textures of Liquid Crystals*, vol. 301, no. 1. Weinheim: WILEY - VCH, 2003.

[90] R. A. Carlton, *Pharmaceutical Microscopy*. Springer, 2011.

[91] B. Fultz and J. Howe, *Transmission Electron Microscopy and Diffractometry of Materials*, 4th ed., vol. 1, no. 11. Berlin: Springer, 2010.

[92] D. B. Williams and C. B. Carter, *Transmission Electron Microscopy: A Textbook for Materials Science*, vol. V1–V4. 2009.

[93] Anton Paar GmBH, "EKA - Electro Kinetic Analyser." [Online]. Available: http://asi-team.com/asi team/brookhaven/BI EKA.pdf. [Accessed: 16-Aug-2015].

[94] V. Tandon, S. K. Bhagavatula, W. C. Nelson, and B. J. Kirby, "Zeta potential and electroosmotic mobility in microfluidic devices fabricated from hydrophobic polymers: 1. The origins of charge" *Electrophoresis*, vol. 29, no. 5, pp. 1092–1101, 2008.

[95] R. P. Chhabra, "Non-Newtonian fluids: An introduction" *Rheol. Complex Fluids*, pp. 3–34, 2010.

[96] A. P. Balgude, X. Yu, A. Szymanski, and R. V. Bellamkonda, "Agarose gel stiffness determines rate of DRG neurite extension in 3D cultures", *Biomaterials*, vol. 22, no. 10, pp. 1077–1084, 2001.

[97] Y. S. Pek, A. C. A. Wan, and J. Y. Ying, "The effect of matrix stiffness on mesenchymal stem cell differentiation in a 3D thixotropic gel", *Biomaterials*, vol. 31, no. 3, pp. 385–391, 2010.

[98] M. Sharma, D. Mondal, C. Mukesh, and K. Prasad, “Preparation of tamarind gum based soft ion gels having thixotropic properties”, *Carbohydr. Polym.*, vol. 102, no. 1, pp. 467–471, 2014.

[99] S. Anoopkumar-Dukie, J. B. Carey, T. Conere, E. O’Sullivan, F. N. Van Pelt, and a. Allshire, “Resazurin assay of radiation response in cultured cells”, *Br. J. Radiol.*, vol. 78, no. 934, pp. 945–947, 2005.

[100] L. Segal, J. J. Creely, a. E. Martin, and C. M. Conrad, “An Empirical Method for Estimating the Degree of Crystallinity of Native Cellulose Using the X-Ray Diffractometer”, *Text. Res. J.*, vol. 29, no. 10, pp. 786–794, 1959.

[101] A. Klug and E. Leroy, *X-Ray Diffraction Procedures: For Polycrystalline and Amorphous Materials*, 2nd ed. New York: WILEY - VCH, 1974.

[102] R. Werbowyj and D. Gray, “Optical Properties of Hydroxypropycellulose”, *Macromolecules*, vol. 17, no. 8, pp. 1512–1520, 1984.

[103] S. Beck-Candanedo, M. Roman, and D. G. Gray, “Effect of reaction conditions on the properties and behavior of wood cellulose nanocrystal suspensions”, *Biomacromolecules*, vol. 6, no. 2, pp. 1048–1054, 2005.

[104] J. E. Celis, *Cell Biology - A Laboratory Handbook*, vol. 1. New York: Elsevier.

[105] H. Kargarzadeh, I. Ahmad, I. Abdullah, A. Dufresne, S. Y. Zainudin, and R. M. Sheltami, “Effects of hydrolysis conditions on the morphology, crystallinity, and thermal stability of cellulose nanocrystals extracted from kenaf bast fibers”, *Cellulose*, vol. 19, no. 3, pp. 855–866, 2012.

[106] AZOM, “The Influence of Particle Size, Zeta Potential and Rheology on Suspension Stability,” 2015. [Online]. Available: http://www.azom.com/article.aspx?ArticleID=10221. [Accessed: 09-Nov-2015].

[107] J. Mewis and N. J. Wagner, “Thixotropy”, *Adv. Colloid Interface Sci.*, vol. 148, pp. 214–227, 2009.

[108] H. Barnes, “Thixotropy - A review”, *J. Nonnewton. Fluid Mech.*, vol. 70, no. 97, pp. 1–33, 1997.

[109] P. H. S. Santos, M. a. Carignano, and O. H. Campanella, “Qualitative study of thixotropy in gelled hydrocarbon fuels”, *Eng. Lett.*, vol. 19, no. 1, 2011.

[110] G. Schramm, *A Practical Approach to Rheology and Rheometry*, 2nd editio. Karlsruhe: Gebrueder HAAKE GmbH, Germany, 2000.

[111] D. R. Picout and S. B. Ross-Murphy, “Rheology of biopolymer solutions and gels.”, *ScientificWorldJournal.*, vol. 3, pp. 105–121, 2003.

[112] G. Rheotec, “Introduction to Rheology”, vol. 49, pp. 0–48.

[113] N. Lin and A. Dufresne, “Surface chemistry, morphological analysis and properties of cellulose nanocrystals with gradiented sulfation degrees”, *Nanoscale*, vol. 6, no. 10, pp. 5384–5393, 2014.

[114] E. Lam, K. B. Male, J. H. Chong, A. C. W. Leung, and J. H. T. Luong, “Applications of functionalized and nanoparticle-modified nanocrystalline cellulose”, *Trends Biotechnol.*, vol. 30, no. 5, pp. 283–290, 2012.

[115] G. Altankov, K. Richau, and T. Groth, “The role of surface zeta potential and substratum chemistry for regulation of dermal fibroblasts interaction”, *Materwiss. Werksttech.*, vol. 34, no. 12, pp. 1120–1128, 2003.

[116] M. Roman, S. Dong, A. Hirani, and Y. W. Lee, “Cellulose Nanocrystals for Drug Delivery”, pp. 81–91, 2010.

[117] Z. Hanif, F. R. Ahmed, S. W. Shin, Y. K. Kim, and S. H. Um, “Size- and dose-dependent toxicity of cellulose nanocrystals (CNC) on human fibroblasts and colon adenocarcinoma”, *Colloids Surfaces B Biointerfaces*, vol. 119, pp. 162–165, 2014.

[118] M. P. E. Wenger, L. Bozec, M. a Horton, and P. Mesquida, “Mechanical properties of collagen fibrils.”, *Biophys. J.*, vol. 93, no. 4, pp. 1255–1263, 2007.

[119] J. a J. Van Der Rijt, K. O. Van Der Werf, M. L. Bennink, P. J. Dijkstra, and J. Feijen, “Micromechanical testing of individual collagen fibrils”, *Macromol. Biosci.*, vol. 6, no. 9, pp. 699–702, 2006.

[120] S. Techatanawat, R. Surarit, T. Suddhasthira, and S. O. P. Khovidhunkit, “Type I collagen extracted from rat-tail and bovine Achilles tendon for dental application: A comparative study”, *Asian Biomed.*, vol. 5, no. 6, pp. 787–798, 2011.

[121] P. Angele, J. Abke, R. Kujat, H. Faltermeier, D. Schumann, M. Nerlich, B. Kinner, C. Englert, Z. Ruszczak, R. Mehrl, and R. Mueller, “Influence of different collagen species on physico-chemical properties of crosslinked collagen matrices”, *Biomaterials*, vol. 25, no. 14, pp. 2831–2841, 2004.

[122] A. Bodin, L. Ahrenstedt, H. Fink, H. Brumer, B. Risberg, and P. Gatenholm, “Modification of nanocellulose with a xyloglucan-RGD conjugate enhances adhesion and proliferation of endothelial cells: Implications for tissue engineering”, *Biomacromolecules*, vol. 8, no. 12, pp. 3697–3704, 2007.

[123] V. Kuzmenko, S. Sämfors, D. Hägg, and P. Gatenholm, “Universal method for protein bioconjugation with nanocellulose scaffolds for increased cell adhesion”, *Mater. Sci. Eng. C*, vol. 33, no. 8, pp. 4599–4607, 2013.

[124] J. M. Dugan, R. F. Collins, J. E. Gough, and S. J. Eichhorn, “Oriented surfaces of adsorbed cellulose nanowhiskers promote skeletal muscle myogenesis”, *Acta Biomater.*, vol. 9, no. 1, pp. 4707–4715, 2013.

[125] S. Arola, T. Tammelin, H. Setälä, A. Tullila, and M. B. Linder, “Immobilization-stabilization of proteins on nanofibrillated cellulose derivatives and their bioactive film formation”, *Biomacromolecules*, vol. 13, no. 3, pp. 594–603, 2012.

[126] Y. Zhang, R. G. Carbonell, and O. J. Rojas, “Bioactive cellulose nanofibrils for specific human IgG binding”, *Biomacromolecules*, vol. 14, no. 12, pp. 4161–4168, 2013.

[127] K. a. Mahmoud, K. B. Male, S. Hrapovic, and J. H. T. Luong, “Cellulose nanocrystal/gold nanoparticle composite as a matrix for enzyme immobilization”, *ACS Appl. Mater. Interfaces*, vol. 1, no. 7, pp. 1383–1386, 2009.

[128] V. Incani, C. Danumah, and Y. Boluk, “Nanocomposites of nanocrystalline cellulose for enzyme immobilization”, *Cellulose*, vol. 20, no. 1, pp. 191–200, 2013.

[129] Y. Fuchigami, T. Takigawa, and K. Urayama, “Electrical Actuation of Cholesteric Liquid Crystal Gels”, *ACS Macro Lett.*, vol. 3, pp. 813–818, 2014.

[130] J. A. Kelly, K. E. Shopsowitz, J. M. Ahn, W. Y. Hamad, and M. J. MacLachlan, “Chiral nematic stained glass: Controlling the optical properties of nanocrystalline cellulose-templated materials”, *Langmuir*, vol. 28, no. 50, pp. 17256–17262, 2012.

Annex I

Shear stress is a force F tangentially applied to an area A which induces a movement in the sample, a flow in the viscous component of the material. The velocity of the flow in an applied stress is controlled by the material viscosity. A sinusoidal force is applied, dependent of a frequency f. [110]

Equation 1 $$Shear\ Stress = \tau = \frac{F}{A} \quad (Pa)$$

Strain is the displacement of the particles of the sample when a force or a stress is applied. Is represented by γ and is dimensionless.[112]

When a shear stress is applied, the upper layers of the sample flow at a maximum velocity v_{max}, in contrast with the bottom layer that remains at rest, that is, with a zero velocity. The velocity of the movement of each layer proportionally decreases with the distance of the layer where the shear stress is applied [112]:

Equation 2 $$Shear\ rate = \dot{\gamma} = \frac{v}{d} \quad (s^{-1})$$

Figure 1, demonstrates the movement of the sample when a parallel plate assay is performed:

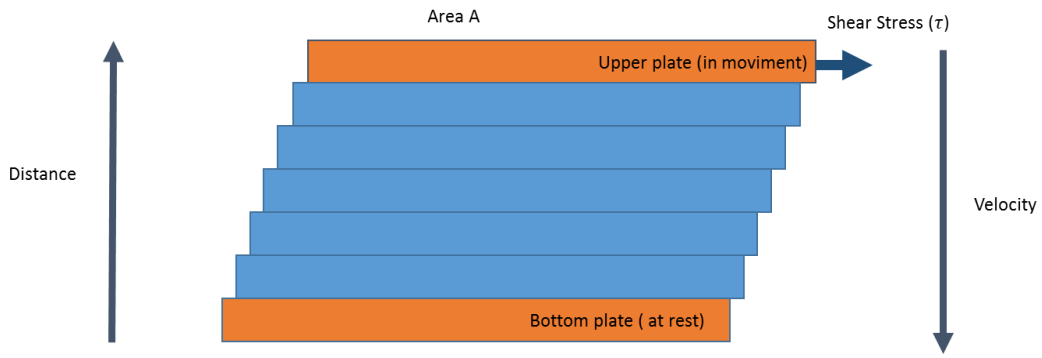

Figure A1 – Schematic of the sample response to an applied shear stress. Adapted from [112].

Many variables influence the viscosity of a material such as: temperature, shear rate, time, pressure and the chemical composition and the pH of the sample. The dynamic viscosity of the material can be obtained by [112]:

Equation 3 $$Dynamic\ viscosity = \eta = \frac{\tau}{\dot{\gamma}} \quad (Pa.s)$$

The material can also be characterized by its viscoelasticity properties which includes the complex shear modulus (G^*) and its components: the storage modulus and the loss modulus:

Equation 4 $$Complex\ Shear\ Modulus = G^* = \frac{\tau^*}{\gamma} \quad (Pa)$$

The complex shear modulus has two components: the shear storage modulus or elastic modulus (G') and the shear loss modulus or viscous modulus (G''). They are related by the phase angle,δ, which is the phase between the sinusoidal stress applied (shear stress) and the sinusoidal answer of the material. [111]

Equation 5: $$G' = G^* \cos\delta \quad (Pa)$$

Equation 6: $$G'' = G^* \sin\delta \quad (Pa)$$

Equation 7: $$\tan\delta = \frac{G''}{G'}$$

The transition from a solid state to a liquid state of a material can be inferred from the G' and G'' values and, consequently, in the phase angle. A solid state sample has a higher G' than G'' and δ <45°. When δ =45° the transition solid-liquid occurs and G'' is higher than G'. [111]

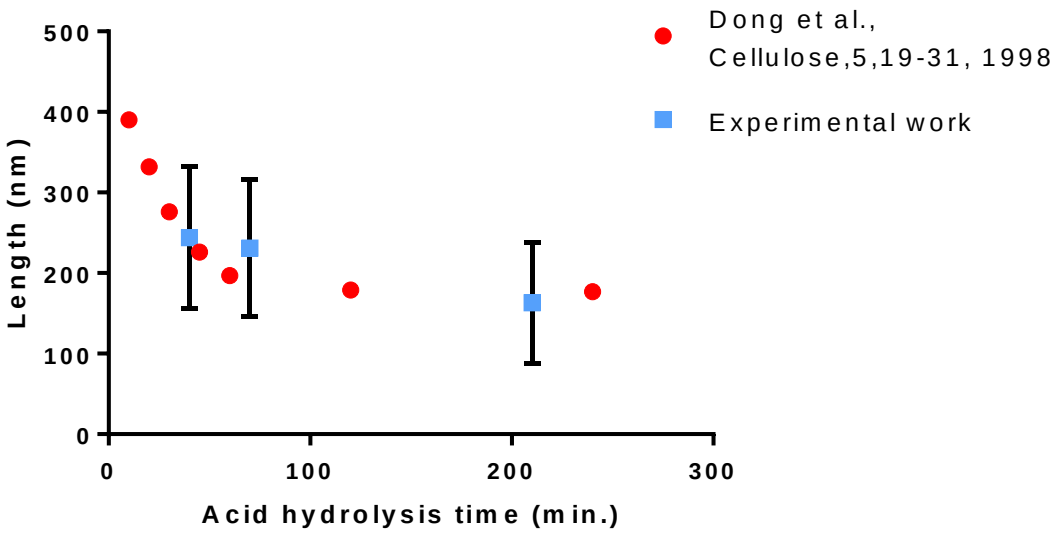

Figure A2 – Graphic of NCC's length versus acid hydrolysis time and comparison with the data from literature [5].